1972

Impulse Voltage Breakdown Strength vs. Temperature of Octafluoropropane (Ca Fa) Gas Exposed to Uniform and Non-uniform Fields

Dinesh N. Taneja

IMPULSE VOLTAGE BREAKDOWN STRENGTH VS. TEMPERATURE OF OCTAFLUOROPROPANE (C_3F_8) GAS EXPOSED TO UNIFORM AND NON-UNIFORM FIELDS

BY

DINESH N. TANEJA

A thesis submitted in
partial fulfillment of the requirements for the
degree Master of Science, Department of
Electrical Engineering, South
Dakota State University

1972

IMPULSE VOLTAGE BREAKDOWN STRENGTH VS. TEMPERATURE OF OCTAFLUOROPROPANE (C_3F_8) GAS EXPOSED TO UNIFORM AND NON-UNIFORM ELECTRIC FIELDS

This thesis is approved as a creditable and independent investigation by a candidate for the degree, Master of Science, and is acceptable as meeting the thesis requirements for this degree, but without implying that the conclusions reached by the candidate are necessarily the conclusions of the major department.

Thesis Advisor Date

Head, Electrical Engineering Department Date

ACKNOWLEDGEMENT

The author gratefully thanks Professor M.L.Manning for his generous assistance in directing and editing this thesis. Also the assistance given by Dr. James Bruce is acknowledged. The financial support given to the author by the Center for Power System Studies was most sincerely appreciated.

TABLE OF CONTENTS

LIST OF FIGURES

CHAPTER I

INTRODUCTION

Use of gas as an insulator is as old as the electrical industry. Earlier electrical apparatus depended heavily on air as an insulating medium. With the development of electrical industries, need arose for better insulating gases than air. The need mainly arose to develop gases with better dielectric strength and thermal conductivity resulting in compact and more efficient designs. The gases also competed with the liquid and solid dielectrics for the same reasons. Generally, the trend to higher voltages with lighter, more compact equipment has helped to increase the use of gaseous insulation. Uses of gases for insulation purposes received a strong impetus upon the development of apparatus with more stringent operating gradients.

Hydrogen has been used to some extent due to its excellent heat transfer characteristics and lower density, but its flammability has been a major limitation for its wide acceptance. The low dielectric strength of Nitrogen rules out its use for some applications. The gases which have invoked a considerable interest in the last three decades are so-called "electronegative gases." They are called "electronegative gases" because of the ability of their molecules to capture free electrons which results in the formation of relatively immobile, negatively charged ions. The absence of highly mobile electrons increases their dielectric strength considerably. The important gases from the insulation point of view, belonging to this category are: Octafluoropropane

(C_3F_8), Octafluorocyclebutane (C_4F_8), Perfluorobutane (C_4F_{10}), and Sulfur Hexalfluoride (SF_6).[1] The fluorocarbon gases generally are thermally more stable than Sulfur Hexafluoride. Generally, Sulfur Hexafluoride is not recommended where operating temperature may exceed 150°C. Some of the fluorocarbon gases have the tendency to decompose under the influence of corona or an arc. However, Sulfur Hexafluoride possesses outstanding current-interrupting ability as compared with the fluorocarbon gases. Sulfur Hexafluoride is very popular for use as an arc-quenching medium in high voltage circuit breakers. Fluorocarbon gases, particularly C_3F_8 and C_4F_8 are extensively used in dry type sealed transformers.

The most important gas of fluorocarbon gases is Octafluoropropane (C_3F_8) which is commercially known as Perfluoropropane, meaning fully fluorinated. The following lists some of the characteristics of Octafluoropropane as an insulating gas.

1. It possesses high dielectric strength at lower pressures.
2. Non-flammable and it does not support combustion, therefore can be used in hazardous places.
3. Low boiling point (-37°C), can be used in apparatus for colder climates without giving trouble after prolonged shutdown.
4. Good heat transfer characteristics, results in compact design of apparatus.
5. Chemically and thermally stable under operating conditions.
6. Non-toxic.

The following is the molecular structure of Octafluoropropane:

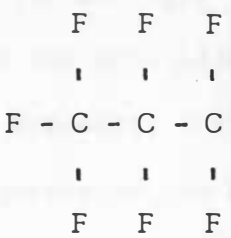

Its physical and chemical properties are:[5]

Molecular Weight	188.02
Normal Boiling Point	-36.7°C
Freezing Point	-160°C
Critical Temperature	71.9°C
Critical Density	0.6 gm/cc
Critical Pressure	26.4 atmos.
Vapor Pressure at 70°F	114.8 psia.
Thermal Stability	Does not decompose at temperatures less than 500°C.
Chemical Stability	Shows negligible corrosion in contact with glass silicon or mild steel and silicone rubber.
Flammability	Non-flammable and does not support combustion.
Toxicity	Non-toxic.
Coefficient of Thermal Conductivity (calculated) at 70°F .	3.6 x 10 cal/sec-cm-°C
Specific Heat (calculated-ideal gas) at 90°C	39.60 cal/gm. mole
Heat of vaporization at 20°C . .	-3.61 K cal/gm. mole

Octafluoropropane gas is used in dry type sealed transformers in network as well as distribution type transformers.[1] Particularly, it is of value in hazardous and semi-hazardous locations. In the design of a transformer, it is necessary that it is corona free. Other possible uses are found in compressed gas substations and transmission lines, wave guides and choppers.

M. L. Manning, in his paper entitled Experience with the AIEE Subcommittee Tests Cell for Gaseous Insulation,[6] has given some of the electrical properties of Octafluoropropane as well as of other gases. The tests give the rapidly applied 60 Hz voltage breakdown strength and one minute withstand voltage test breakdown strength. Four types of electrode systems were used. These results were conducted at room temperatures and pressure. The impulse voltage breakdown strength of the gas was given by L. C. Whitman in his paper entitled Impulse Voltage Tests on Air and C_3F_8.[7] The impulse breakdown strength is given for $1\frac{1}{2} \times 40$ μsec impulse waveshape using two types of electrode systems. These tests were conducted at room temperature and pressure. In an earlier investigation in this department, Edward Roman in his thesis entitled Voltage Breakdown Strength vs. Temperature of Octafluoropropane Gas Exposed to Uniform and Non-uniform Field,[8] has given results of 60 Hz rapidly applied and one minute voltage withstand breakdown strength tests on Octafluoropropane gas up to 200°C. Two types of electrode systems were employed in his work.

Purpose of the thesis: The purpose of my thesis is to investigate the impulse voltage breakdown strength of Octafluoropropane gas as a function of the temperature of the gas. The standard 1.5 x 40 μsec. positive polarity impulse waveshape was used in all the tests. The investigation was made with and without a weak source of irradiation present near the cell. Two types of electrode systems were used: three-fourth inch sphere to grounded plane which represented a fairly uniform field, and a point to grounded plane representing a highly non-uniform field. The tests were carried out from room temperature to a temperature of 150°C. The impulse ratios of the gas was also plotted using some of the data from Roman's thesis.[8] Impulse Ratio is defined as the ratio of the impulse crest voltage strength and the crest value of 60 Hz one minute voltage withstand test. It is a very important factor for designers from an insulation co-ordination point of view.

CHAPTER II

REVIEW OF LITERATURE

Much work has been done for electrical breakdown characteristics of electronegative group of gases. The pioneer work in this area was published by Messrs G. Camilli, R. E. Plump, J. D. Corbine, C. N. Works and T. W. Dakin,[2,3,4] as well as by other researchers. However, in the literature one does observe the inconsistency of many test methods used and also in the several types of electrode systems employed. In the past, investigators have used several types of electrode systems which were sphere to sphere (with varying diameters), sphere to rod, sphere to plane, plane to plane, rod to plane, rod to rod, etc. This resulted in the difficulty in comparing the datas given in different papers.

M. L. Manning in his paper entitled Experience with the AIEE Subcommittee Test Cell for Gaseous Insulation,[6] gave recommendations regarding the types of electrode systems to be used for gaseous evaluation. He used four types of electrode systems: Electrode System A 3/4" diameter brass sphere to 1-3/4" diameter brass plane, Electrode System B 1/2" square brass rod to 1-3/4" diameter brass plane, Electrode System C 3/4" diameter brass sphere to a 1" square projected brass rod, and finally Electrode System D, a 1/2" square brass rod to a 1" square projected brass rod. To obtain consistent results, use of a 0.9 megohms resistor was suggested for 60 Hz voltage tests. For impulse voltage tests solid grounding of the bottom electrode was recommended. The

results of the 60 Hz rapidly applied voltage breakdown tests conducted on C_3F_8, SF_6, N_2, and Air under uniform field conditions at room temperature and pressure showed that C_3F_8 had a breakdown strength 1.87 times that of air for 0.1" gap spacing and 2.25 for 0.5" gap spacing. For one minute voltage withstand test, the ratio of the breakdown strength of C_3F_8 to air, under uniform field conditions was found to be 2.09 at 0.1" gap spacing to 2.25 at 0.5" gap spacing. The same tests were conducted to evaluate the positive polarity impulse breakdown strength of the gases. The desirability of using more than one set of electrode systems in the cell to obtain varying kinds of electric fields was suggested by M. L. Manning for the evaluation and comparison of the voltage breakdown strength of various gases.

In another paper, M. L. Manning and E. D. Padgett[1] studied the 60 Hz voltage breakdown strength of C_3F_8, SF_6, N_2 and air using a test cell with and without a directly grounded bottom electrode. Impulse Voltage breakdowns of mixture of C_4F_8, N_2 and C_3F_8 was also studied. The need for standardization of the test cell and kinds of electrode systems was strongly demonstrated by these investigators.

L. C. Whitman in his paper entitled Impulse Voltage Tests on Air and C_3F_8,[7] compared the impulse voltage breakdown strength of C_3F_8 and air. Two types of electrode system were used: a 1" diameter brass sphere to a 1-3/4" diameter square-edged brass plane, and a 3/32" diameter tungsten rod, with a 25° sharp point to a 1-3/4" diameter square-edged brass plane. All the tests were conducted at room

temperature and pressure. The impulse breakdown with both positive and negative polarity impulses of 1-1/2 x 40μsec waveshape was discussed. His results showed that for the sphere to plane electrode system, the breakdown voltage ratio of C_3F_8 to air for positive polarity impulse varied from 3.30 at a 0.05" gap spacing to 2.50 at 0.35" gap spacing, and finally to a ratio of 3.0 at 0.75" gap spacing. For the same kind of electrode system, with negative polarity impulse voltages, this ratio varied from 2.54 at 0.25" gap spacing to 2.60 at a 0.50" gap spacing and finally to 2.7 at a 0.63" gap spacing. For positive polarity, the ratio varied from 2.50 at a 0.5" gap spacing to 2.35 at 1.0" gap spacing for point to plane electrode systems. For negative polarity impulse, using the same electrode system, the ratio varied from 4.85 to a 0.4" gap spacing to 2.5 at a 0.9" gap spacing.

In comparison with the research devoted to other aspects of voltage breakdown phenomena, relatively lesser attention has been given to the effects of high temperatures on the breakdown strength of gaseous insulation. Alston[9] studied the effects of high temperatures on direct current voltage flashover in air. Paschen's Law was confirmed for temperatures up to 1100°K in air under uniform field conditions. Paschen's Law states that the voltage breakdown of the gas in a uniform field is proportional to the product of the electrode gap spacing and the pressure of the gas. Alston[9] found the flashover value of air to be independent of electrode material. The electric breakdown strength was inversely proportional to the absolute temperature for temperatures up

to 1100°C. He concluded that hot spots on electrode surface under uniform field conditions reduce the breakdown strength of air. Under non-uniform field conditions this effect was found to be less.

Sharbaugh, Watson, White, Lee and Greenwood[10] studied the breakdown strength of Nitrogen at high temperatures using a shock tube. Temperatures as high as 4,000 K° and gas velocities as high as 2,500 m/sec were attained by using a shock wave to heat and accelerate the gas between a pair of electrodes located inside the shock tube. It was concluded that d.c. voltage breakdown strength of N_2 at 4,000°K decreases to half of its room temperature value. This drop in breakdown strength at high temperatures was attributed to a thermally ionized condition of the gas. At 4,000°K, remarkably high pre-breakdown currents were observed. Paschen's Law was found to hold true for temperatures up to 1,100°K. These tests were conducted under a non-equilibrium gas state whereas it would have been more desirable to determine results under an equilibrium gas state for fundamental work.

Roman[8] carried out an investigation to evaluate the 60 Hz voltage breakdown strength of C_3F_8 gas for temperatures up to 200°C. The phenomena was studied under uniform as well as under non-uniform field conditions. The voltage breakdown strength of C_3F_8 was found to decrease slightly or remain constant as the temperature was increased, both in presence as well as in absence of a weak irradiation source. Under non-uniform field conditions, the voltage breakdown strength, with or without irradiation, was found to decrease with temperature.

CHAPTER III

BASIC THEORY

The following is the list of the symbols used in the derivation of various equations to represent the phenomena of electric discharges through gases:

α = Townsend's first ionization coefficient

n_o = number of electrons emitted per second from cathode

d = distance between cathode and anode

x = distance of the small lamina considered from the cathode

d_x = thickness of the small lamina

E = electric field strength

n_x = number of electrons passing through the lamina per second

n_d = number of electron reaching the anode per second

I_o = initial current through the gas due to irradiation and photons

I = current through the gas

n_o' = number of secondary electrons produced per second at cathode

n_o'' = total number of electrons per second leaving the cathode

γ = Townsend's second ionization coefficient

The groundwork for general theory of electric discharges through gases was laid by Townsend and his co-workers between 1900 and 1920.[11,12,13] In the following years, the Townsend's theory of electric discharges was improved and extended. The most important extension work

was done by Loeb and Meek,[12] who proposed streamer theory of electric discharges in 1936. The original Townsend's theory is applicable for electrical discharges at lower pressures (far below atmospheric pressures), whereas the streamer theory is applicable at higher pressures. The Townsend's theory of electrical discharges has two regions, Pre-Spark characteristics and Townsend's criterion for spark breakdown.

A. Pre-Spark Characteristics

The typical pre-spark volt-ampere characteristics of any gas placed between two electrodes which produces a fairly uniform field condition, is shown in Fig. 1. It is obtained by increasing the anode to cathode voltage from zero to higher values until breakdown of the gas occurs. The volt-amperes characteristics considered here are for constant external irradiation and for a low gas pressure.

As the magnitude of the applied voltage is increased from zero, the current through the gap increases slowly. The current in the gap is due to the movement of already existing ions and electrons. These free electrons and ions are present because of external irradiation or photons, etc. Since the current is very small, it will not upset the equilibrium. Its value will be proportional to electrons velocity and the applied voltage. The mobility of electrons is nearly constant. Therefore, the current will be proportional to the applied voltage only. The gas acts like an ohmic conductor from point O to point A on the characteristics curve on Fig. 1. This portion is called a space charge limited region.

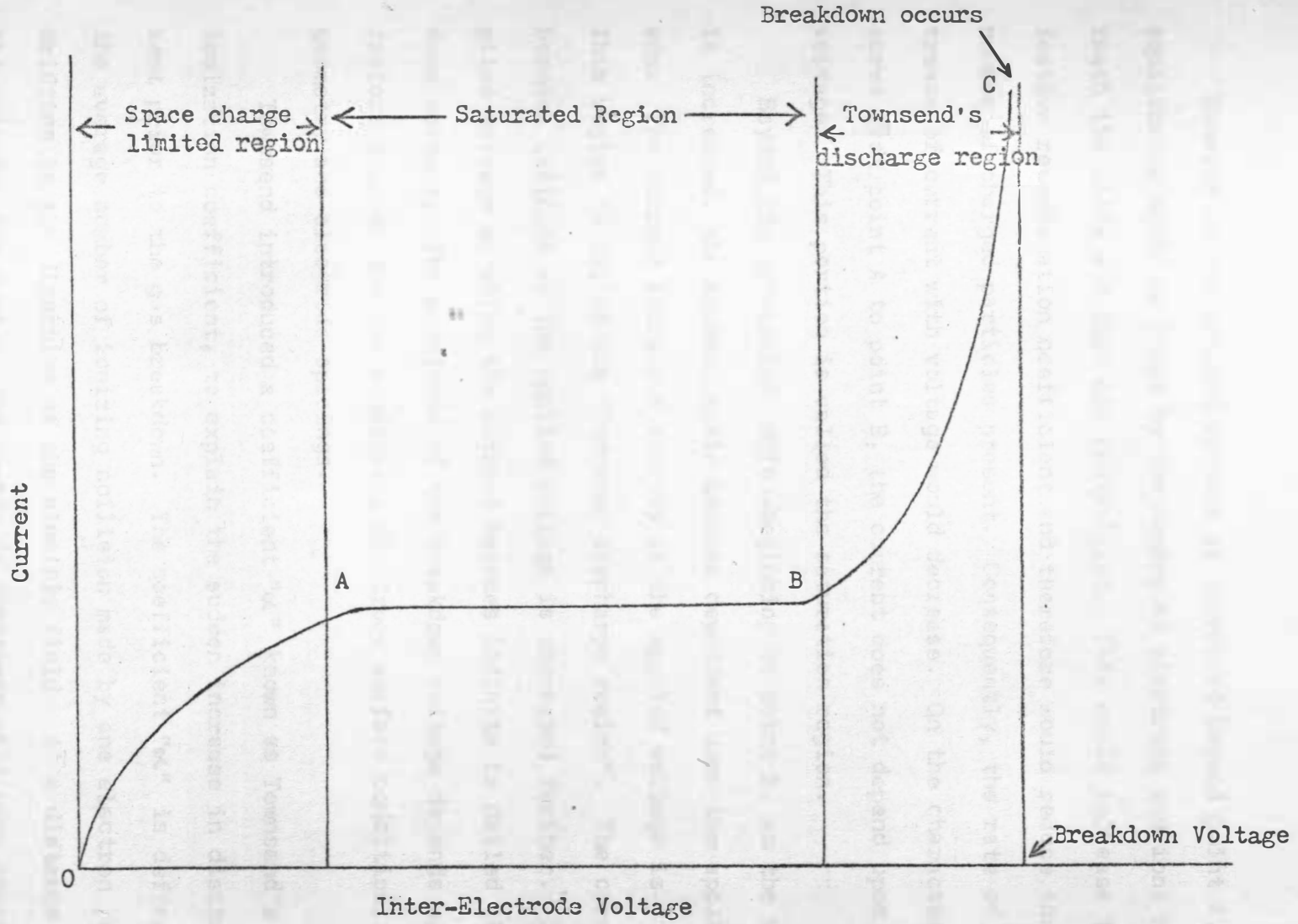

Fig.1 Pre-Spark Volt-Ampere characteristics of a gas between two electrodes.

However as the applied voltage is increased beyond point A, the equilibrium would be upset by the number of electrons and ions which reach the anode and then are neutralized. This would increase the effective recombination coefficient and therefore would reduce the total number of charged particles present. Consequently, the rate of increase of current with voltage would decrease. On the characteristics curve from point A to point B, the current does not depend upon the voltage. This portion is called the saturation region.

Beyond the saturation region beginning at point B, as the voltage is increased, the current again becomes dependent upon the applied voltage. The current increases sharply as the applied voltage is increased. This region is called the "Townsend discharge region". The current becomes infinite as the applied voltage is increased further. The applied voltage at which the current becomes infinite is called the breakdown voltage. The magnitude of the breakdown voltage depends upon many factors such as the gas condition, electrode surface condition, and geometry and electrode spacings.

Townsend introduced a coefficient "α" known as Townsend's first ionization coefficient, to explain the sudden increase in discharge current prior to the gas breakdown. The coefficient "α" is defined as the average number of ionizing collision made by one electron per cm. drifting in the direction of the electric field. At a distance x from the cathode, the number, the number of electrons will have increased from n_o to n_x by ionizing collisions. These n_x electrons, in traversing

the lamina d_x at x in the direction of the field E, will generate, by ionizing collisions, new electrons and positive ions, such that

$$dn_x = \alpha\, n_x dx \tag{1}$$

In the above relation, recombination and diffusion is neglected.

By integrating from cathode to the plane, we get

$$\int_{n_o}^{n_x} \frac{dn_x}{n_x} = \int_{o}^{n} \alpha\, dx$$

or, if α is independent of x

$$n_x = n_o\, e^{\alpha x} \tag{2}$$

Therefore, the number of electrons striking the anode per second n_d at x = d will be given by

$$n_d = n_o\, e^{\alpha d} \tag{3}$$

i.e., on the average, each electron, leaving the cathode, produces $(e^{\alpha d} - 1)$ new electrons and positive ions before reaching the anode.

The current in the gas is due to the movement of electrons and positive ions in the gap. In the steady state, the number of positive ions reaching the cathode per second just equals to the number of newly formed electrons reaching the cathode, so that the current will be given by

$$I = I_o\, e^{\alpha d} \tag{4}$$

The above equation gives a steady state relation value of the current. The current does not represent a self sustained discharge since it depends upon I_o.

The current growth equation, with secondary mechanism, was derived by Townsend by introducing a second ionization constant "γ". It is defined as the average number of secondary electrons produced at the cathode per ionizing collision in the gap.

The total number of electrons per second leaving the cathode would be the sum of number of electrons emitted per second from cathode and number of secondary electrons produced per second at cathode.

$$n_o'' = n_o + n_o' \tag{5}$$

Each electron leaving the cathode produces $(e^{\alpha d} - 1)$ collisions in the gap, therefore, the number of ionizing collisions per second in the gap will be equal to $n_o(e^{\alpha d} - 1)$, and by definition of γ ,

$$n_o' = \gamma n_o'' (e^{\alpha d} - 1) \tag{6}$$

Substituting the value of n_o' in equation (6)

$$n_o'' = n_o + n_o'' (e^{d} - 1) \tag{7}$$

or

$$n_o'' = \frac{n_o}{1 - \gamma(e^{\alpha d} - 1)} \tag{8}$$

from equation (3), the number of electrons reaching the anode is given by

$$n_d = n_o'' e^{\alpha d} \tag{9}$$

so that

$$n_d = \frac{n_o e^{\alpha d}}{1 - \gamma(e^{\alpha d} - 1)} \tag{10}$$

In the steady state, the current in the gap will be given by

$$I = \frac{I_o e^{\alpha d}}{1 - \gamma(e^{\alpha d} - 1)} \tag{11}$$

The current therefore increased from its previous value by virtue of the term $\gamma(e^{\alpha d} - 1)$ which becomes significant for higher value of d. The value of γ, which varies widely and is always less than unity, depends upon the nature of the gas as well as on the electrode material. In the derivation of the above relation, the effect of attachment is neglected. The process in which an electron, colliding with a neutral particle, forms a negative ion is called attachment. The attachment effect would tend to reduce the value of current at higher value of electrode separation because of loss of electrons by attachment.

B. Townsend's Criterion for Spark Breakdown

Equation (11) shows that the value of the current would become theoretically infinite if

$$1 - \gamma(e^{\alpha d} - 1) = 0 \tag{12}$$

On the characteristic curve, this represents the sudden increase in the current to a very high value. The above equation, therefore, forms a breakdown criterion. Equation (12) can be rewritten as

$$\gamma e^{\alpha d} = \gamma + 1 \tag{13}$$

or, since $\gamma << 1$

$$\gamma e^{\alpha d} = 1 \qquad (14)$$

This is known as the Townsend's criterion or the sparking criterion. Since the above equation does not depend upon irradiation and presence of photons, we have a self sustaining discharge.

C. Streamer Theory of Breakdown

The branched and irregular growth of sparks in long gaps was difficult to reconcile with the Townsend's theory. Loeb and Meek[12] proposed the streamer theory of spark for positive streamers. Raether[12] proposed streamer theory from negative streamer independently. The streamer theory essentially describes the spark discharge from a single avalanche which in itself transfers into streamers resulting in the breakdown.

The positive streamer from the anode as originally developed by Loeb and Meek[12] under uniform field conditions is explained as follows: An avalanche is initiated by a free electron's collision with a gas molecule. The electron ionizes the gas molecules and also produces excited atoms. These excited atoms give of photons which in turn ionize more molecule and also produce more electrons. As a consequence, it results in large amounts of photoionization of gas molecules in the space ahead of the streamer and the large local enhancement of the electric field by the ion space charge at the tip of the streamer. The space charge produces a distortion of the field in the gap. The positive ion may be assumed immobile as compared with the rapidly moving

electrons. The avalanches develop across the gap as a cloud of electrons leave the positive ions space charge behind.

When the avalanche crosses the gap, the electrons are swept across the gap as shown in Fig. 2(a). The ion density is low except for the highly localized space charged field produced near the anode. Therefore, the presence of the positive ions alone does not in itself constitute breakdown in the gap.

The electrons produced by the photons emitted from the densely ionized gas initiate auxiliary avalanches which again are directed toward the main avalanche. The greatest multiplication in these auxiliary avalanches occur along the axis of main avalanche. This is because of the fact that the space charge field is supplemented by the external field. Positive ions are left behind and the process develops as a self-propagating streamer as shown in Fig. 2(b). The streamer forms a conducting filament of highly ionized gas between the electrodes as shown in Fig. 2(c). A backstroke develops and breakdown follows. On very long gaps, the streamer may not reach the cathode at all. A number of secondary streamers may develop which too may not reach the cathode and the breakdown does not occur under this case.

D. Breakdown in Electronegative Gases

The electronegative gases are characterized by the ability of their molecule to capture free electrons to form relatively immobile negatively charged ions.[20] Since negative ions like positive ions are too massive for producing collisional ionization, attachment represents an

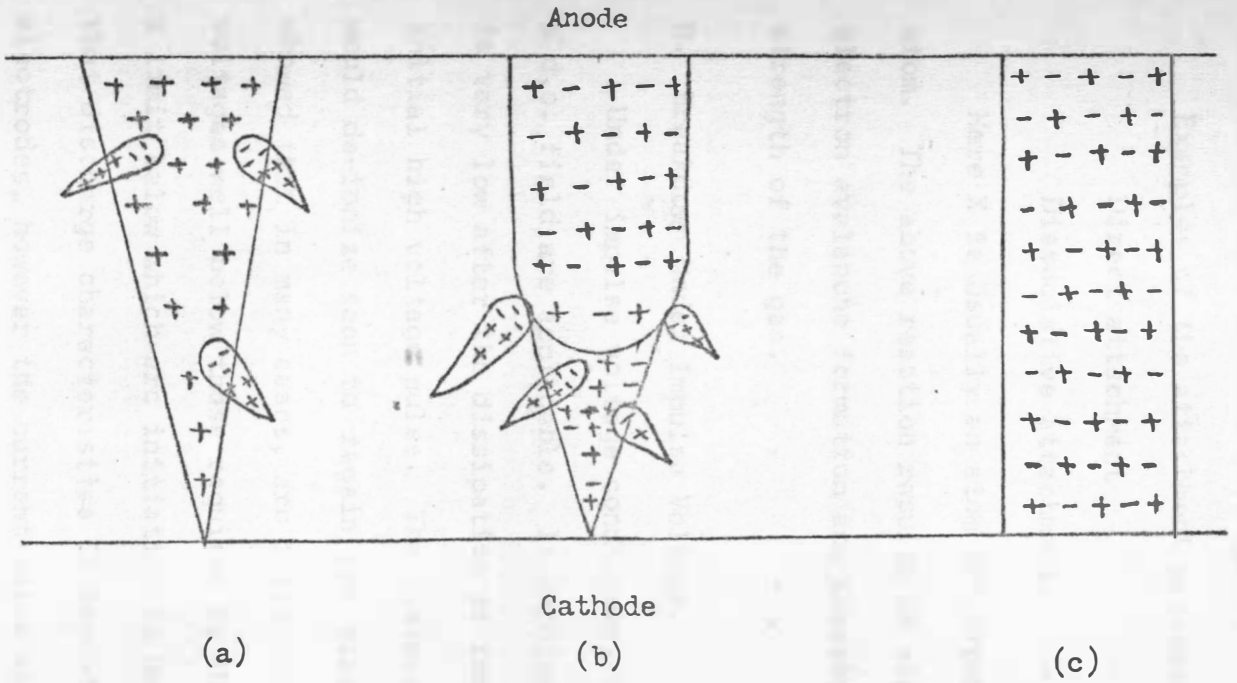

Fig.2 Cathode-directed streamer.

effective way of removing free electrons which otherwise would have contributed to avalanche development.

Examples of the attachment processes are:

Direct attachment $- XY + e \rightarrow XY^-$

Dissociative attachment $- XY + e \rightarrow X + Y^-$

Here X is usually an atom of carbon or sulfur and Y is a halogen atom. The above reaction results in electron capture, thus preventing electron avalanche formation and thereby increasing the dielectric strength of the gas.

E. Breakdown Under Impulse Voltage

Under impulse voltage conditions, the breakdown characteristics of a d.c. field are applicable. In impulse voltage breakdown, the current is very low after the dissipation of the energy associated with the initial high voltage pulse. The discharge is then unstable and the gas would de-ionize soon to regain its dielectric strength. Alston[14] showed that in many cases, arc initiation may occur at values of applied voltages well below those required by the slow criterion, but there is a limit below which arc initiation is not possible. He also indicated that discharge characteristics is dependent upon the condition of the electrodes, however the current value was always in the range of 0.1 to 0.7 amperes.

CHAPTER IV

EQUIPMENT

A. Impulse Voltage Test Set

The full wave impulse voltages were obtained from a Westinghouse portable impulse generator with maximum output rating of 125 kV. The generator uses a three stage Marx parallel charge series discharge capacitor circuit. It consists essentially of three condensers, spark gaps and resistors connected such that the condensers are charged from a relatively low voltage d.c. source and are discharged in series to give a high voltage pulse of short duration across the test piece. Upon triggering, mechanically, by an electric motor, the first set of spheres were shorted. This would cause the remaining two sphere gaps to breakdown across their air gaps. Thus, the triggering would put all the three charged capacitors to discharge in series through the test object as shown in Fig. 3. The discharge voltage at the output terminal would be slightly less than three times the voltage across single condenser. This is due to voltage drops across the internal sphere gaps and the wave shaping resistor.

The charging equipment consisted of a step-up transformer and selenium rectifier unit. The charging voltage could be varied smoothly from zero to maximum by means of a voltage regulator in the primary circuit of the step-up transformer. The control knob of this regulator was located on the control cabinet panel. The condenser of each stage of the generator consisted of a large number of askarel impregnated

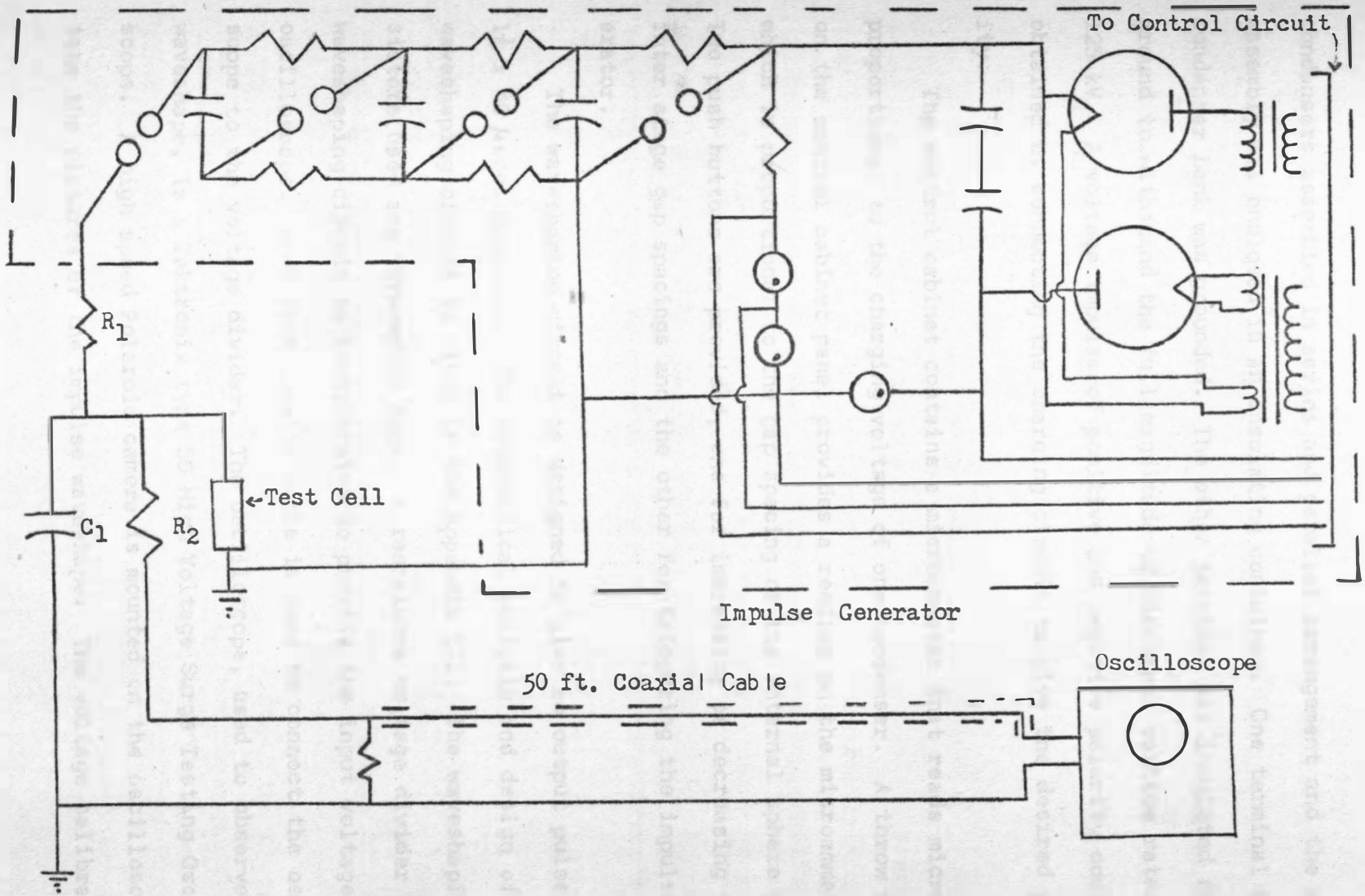

Fig.3 Impulse Generator and Wave Shaping Circuit Diagram.

condensers assembled in series and parallel arrangement and the whole assembly was enclosed in an insulating container. One terminal of the condenser bank was grounded. The other terminal was insulated from ground to withstand the full magnitude of discharge voltage rated at 125 kV. A voltage impulse of positive and negative polarity could be obtained by connecting the charging circuit to give the desired polarity.

The control cabinet contains a microammeter that reads microamperes proportional to the charging voltage of one condenser. A throw switch on the control cabinet panel provides a reading on the microammeter which is proportional to the gap spacing of the internal sphere gaps. Two push buttons are provided, one for increasing or decreasing the inter stage gap spacings and the other for triggering the impulse generator.

The waveshaping circuit is designed to give an output pulse of $1\frac{1}{2} \times 40\ \mu$sec. duration. The mathematical analysis and design of the waveshaping circuit is given in the Appendix III. The waveshaping resistors used are wire-wound type. A resistance voltage divider in the waveshaping circuit is incorporated to provide the input voltage to the oscilloscope. A 40 foot coaxial cable is used to connect the oscilloscope to the voltage divider. The oscilloscope, used to observe the waveshape, is a Tektronix type 50 High Voltage Surge Testing Oscilloscope. A high speed Polaroid camera is mounted on the oscilloscope to take the pictures of the impulse waveshape. The voltage calibration

of the control panel meter is accomplished by the oscilloscope as well as by 6.25 cm. diameter sphere gaps, as given in Appendix IV. A control circuit is employed for synchronization of tripping of the impulse generator with the oscilloscope. The impulse generator and the wave-shaping circuit are shown in Fig. 3.

B. Gas Test Cell

Two types of test cells were used in the testing of the gas. Both cells were manufactured by Messrs. M. J. Seavy and Sons, New York. The test cells were designed and manufactured as par recommendations of ASTM Standards-part 29. These specifications and recommendations were approved by Section III of the Electrical Test Committee N of ASTM Committee D-27 on Electrical Insulating Liquids and Gases.[18] Round-Robin tests on dielectric strength of gases by use of three different test cells were made in 1961.[6] The inside features and dimensions of both the cells are shown in Fig. 4 and Fig. 5. The inside volume of both the cells was 20.8 cubic inches.

Each cell has a two inch inside diameter by eight inch long hollow pyrex glass cylinders. On each end of the glass cylinder, an aluminum end ring is attached with a teflon gasket between the glass and the metal ring. The gasket also acts as a cushion between the glass and the ring. On the lower end of the glass cylinder, a cylindrical steel plate is attached, with bolts, which have an attached fixed brass electrode system and a high temperature valve. On the top end of the glass cylinder another cylindrical metal plate of a half-inch thick

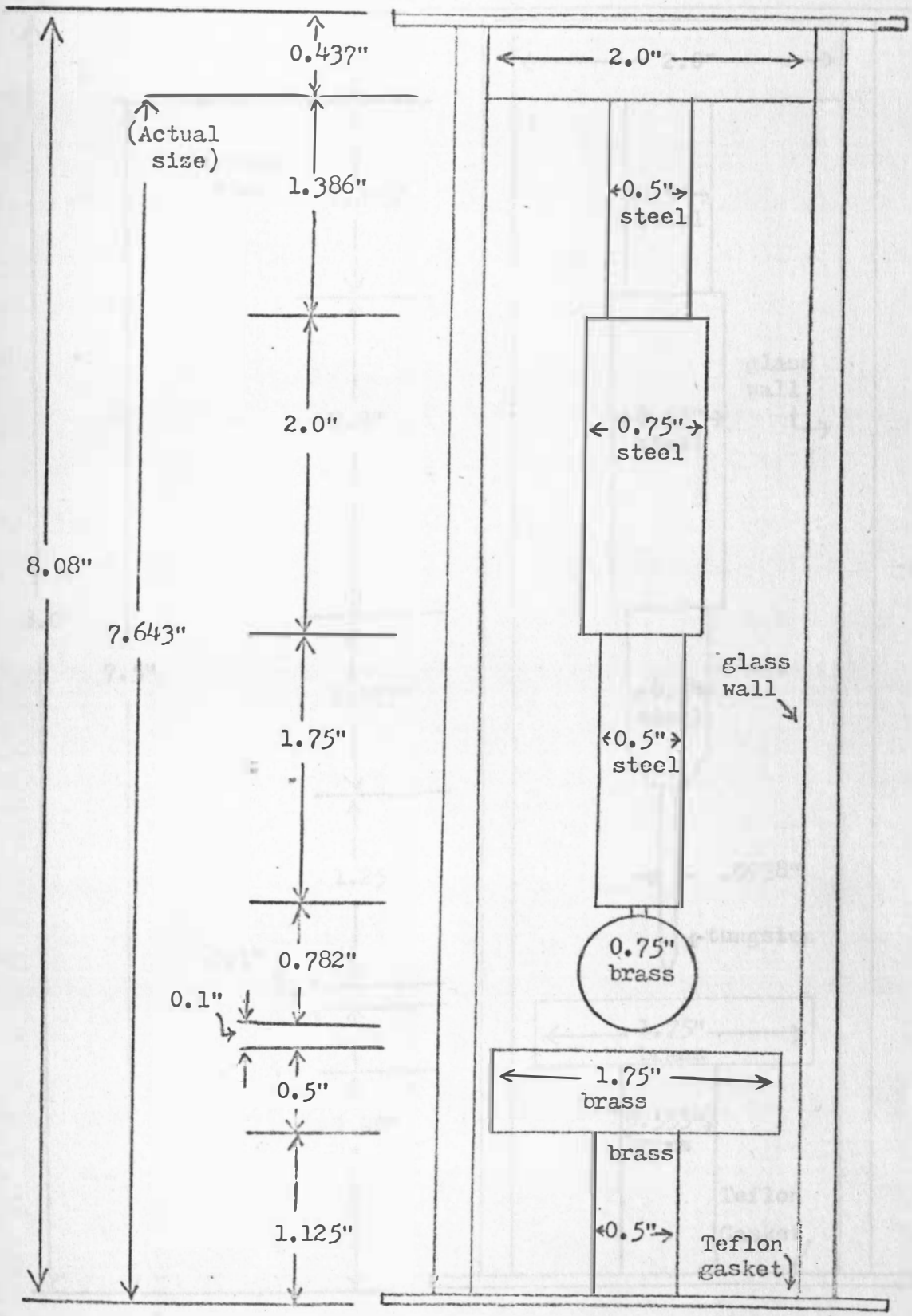

Fig.4 Inside Features of a Sphere to Grounded Plane Test Cell.

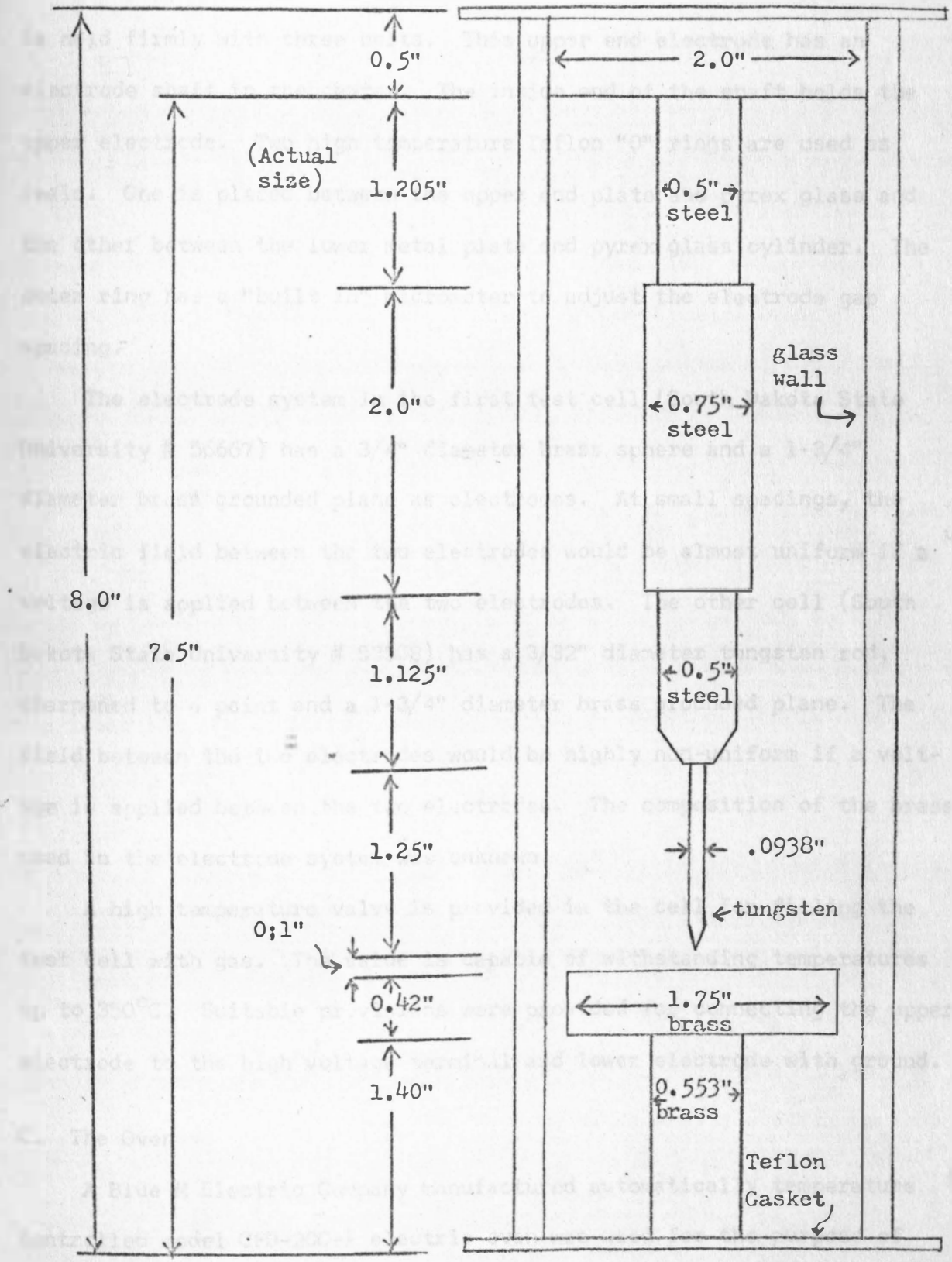

Fig. 5 Inside Features of Point to Grounded Plane Test Cell.

is held firmly with three bolts. This upper end electrode has an electrode shaft in the center. The inside end of the shaft holds the upper electrode. Two high temperature Teflon "O" rings are used as seals. One is placed between the upper end plate and pyrex glass and the other between the lower metal plate and pyrex glass cylinder. The outer ring has a "built in" micrometer to adjust the electrode gap spacing.

The electrode system in the first test cell (South Dakota State University # 56667) has a 3/4" diameter brass sphere and a 1-3/4" diameter brass grounded plane as electrodes. At small spacings, the electric field between the two electrodes would be almost uniform if a voltage is applied between the two electrodes. The other cell (South Dakota State University # 53508) has a 3/32" diameter tungsten rod, sharpened to a point and a 1-3/4" diameter brass grounded plane. The field between the two electrodes would be highly non-uniform if a voltage is applied between the two electrodes. The composition of the brass used in the electrode system was unknown.

A high temperature valve is provided in the cell for filling the test cell with gas. The value is capable of withstanding temperatures up to 350^{o}C. Suitable provisions were provided for connecting the upper electrode to the high voltage terminal and lower electrode with ground.

C. The Oven

A Blue M Electric Company manufactured automatically temperature controlled model CFD-20C-1 electric oven was used for the purpose of

heating the test cell. The automatic control cabinet panel for controlling the desired temperature automatically was manufactured by Honeywell Corporation. The inside dimensions of the oven are 20" high, 20" deep and 24" wide. The oven has a heating range of room temperature to 650°C. The oven is equipped with a blower which continuously circulates the heated air inside the oven. The oven has two portholes, one for high voltage leads and the other for low voltage leads. A cylindrical ceramic insulator, made by the Art Department at South Dakota State University, was used to insulate the incoming high voltage lead from the impulse generator, to the oven from the oven body. The body and frame of the oven was solidly grounded. A gap spacing of 0.1" was used in the test cell. The ceramic insulator was not capable of withstanding impulse voltages higher than about 60 kV. The oven door is equipped with a safety interlock device which disconnects the power supply to the high voltage side of the impulse generator if the oven door is not closed.

D. Source of Ionization

A weak radiation source was used for ionization purposes in some of the tests. The radiation source and its position, relatively, to the test cell was essentially the same as that used by Keith E. Crouch in his thesis entitled "The Effect of Wave Shape on the Electrical Breakdown of Nitrogen Gas",[16] and also by Edward J. Roman in his thesis entitled "Voltage Breakdown Strength vs. Temperature of Octafluoropropane

Gas Exposed to Uniform and Non-Uniform Fields".[8] The source used was a millicurie of radium in a lead can 1.3" thick on the sides. No special precautions were required in the handling of the irradiating source since the irradiation level of the source was lower than safe level as prescribed by U. S. Atomic Energy Commission. The safety check was done by a Geiger Muller Counter. The source was placed at approximately 18-3/4" away from the electrode line of the test cell. It was placed just outside the left wall of the oven. It was found that the oven wall had virtually no effect on the count rate. It was assumed that ionization in the test cell was primarily due to low energy gamma rays since beta rays would not penetrate through the pyrex glass test cell walls.

CHAPTER V

TEST PROCEDURE

A. Method of Cleaning Test Cells

Before any tests were made, the cell was disassembled and the electrodes were prepared (sanded). The lower electrode surface was first sanded with silicon carbide paper of grade 240A followed by grade 320A and finally with grade 500A. The upper electrode was prepared only with the finest grade 500A. All electrodes, except the upper electrode of the point to plane system, were polished on an electric rouge wheel. The preparation of the electrodes was done to remove any pits that might have developed on the electrode surface due to sparkover during impulse testing.

All inside parts of the cell were washed with tap water, thoroughly rinsed with distilled water and finally with acetone. The commercial grade of acetone used acted as a drying agent. The test cell parts were set aside for about two hours to dry and were reassembled again. It was important that after the assembly, the test cell should be perfectly air tight. This was checked prior to filling the cell with gas as described in the method of filling the test cell.

B. Test Cell Gap Spacing Adjustment

The micrometer of the test cell was used in setting the desired gap between the high voltage electrode and the ground electrode. The gap used in all the tests was 0.1". The greater gap spacing would result in higher breakdown voltages. Greater gap spacing was not used

since the ceramic insulator on the high voltage lead inside the oven was not capable of withstanding impulse voltages higher than about 60 kV.

Adjustment of the gap spacing was done by using an ohmmeter. One terminal of the ohmmeter was connected to the high voltage terminal of the cell while the other terminal was connected to its ground terminal. The micrometer was turned down until the high voltage electrode of the test cell just touched the lower ground electrode. Upon contact, the ohmmeter would indicate an almost zero resistance. The zero gap spacing was recorded and 0.1" was added to it. The micrometer was adjusted to this new reading.

The gap spacing would decrease at temperatures higher than room temperatures due to expansion of various test cell parts. Since most of the tests were conducted at temperatures higher than room temperature, a method as given in Appendix VI was employed to offset the decrease in the gap spacing. The amount by which the test cell gap decreases can be calculated from the data given in Table II. The temperature at which the impulse voltage test is to be conducted is known. The micrometer was again adjusted by the amount calculated. Thus, the adjustment would take into account the linear expansion of the electrodes.

C. Method of Filling the Test Cell With Gas

The apparatus used in the filling of the test cells is shown in Fig. 6. The apparatus is basically the same as used by Roman,[8] except for minor changes. After setting the electrode gap spacing, the cell

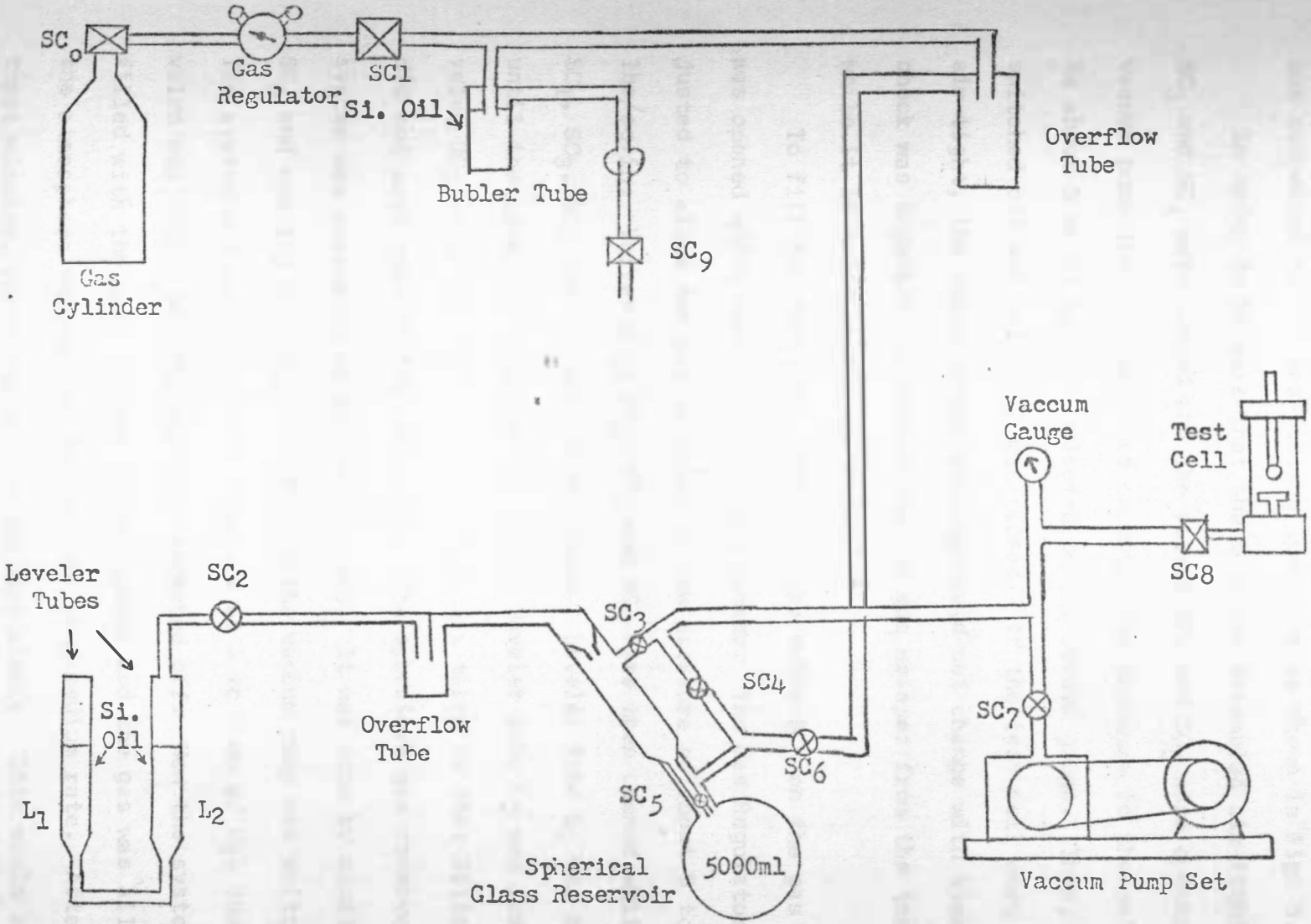

Fig.6 Apparatus Used in Filling the Test Cell with Gas.

was connected to the gas-filling apparatus as shown in Fig. 6.

In order to be sure that the cell was assembled air-tight, valves SC_3 and SC_4 were closed and the valves SC_7 and SC_8 were opened. The vacuum pump then was switched on until the pressure in the cell dropped to about 5 mm of Hg. as indicated on the vacuum gauge. Then, it was switched off and valve SC_7 was closed. If the test cell were assembled air-tight, the vacuum gauge reading would not change with time. This check was necessary to ensure that no gas escapes from the test cell while it is being heated or tested.

To fill the test cell with gas, the valve SC_0 on the gas cylinder was opened while valve SC_1 was kept closed. The Gas Regulator was adjusted to allow the gas to exist at low pressure of about 5 to 7 lbs/sq.in. Valves SC_2, SC_5, SC_6 and SC_9 were then opened while valves SC_1, SC_3, SC_4 and SC_7 were kept closed. Leveler tube L_1 was raised until the level of Silicone Oil in the leveler tube L_2 was just up to valve SC_2 which was then closed. Care was taken so that Silicone Oil did not pass through the valve SC_2. The spherical gas reservoir and the system was evacuated by the vacuum pump. It was done by closing value SC_6 and opening SC_3, SC_4 and SC_7 and the vacuum pump was switched on. The system was evacuated to a pressure of 3 to 5 mm of Hg. and then the valve was closed and the pump was switched off. Now the system was filled with the gas. Valve SC_7 was opened and the gas was allowed into the atmosphere through the bubler tube at a medium rate. After two or three minutes, valve SC_6 was opened very slowly. This would allow the

gas to fill the evacuated system. Valve SC_6 was kept opened until the system was filled with the pressure nearly equal to the atmospheric pressure. Valves SC_6, SC_9 and SC_1 were then closed and the system was evacuated and refilled with the gas as before.

With valves SC_1, SC_6 and SC_7 closed and the system filled the gas, valve SC_2 was slowly opened. Simultaneously, leveler tube L_1 was lowered slightly so that no oil would pass through valve SC_2. If any oil had passed beyond valve SC_2, then the overflow tube was taken out and cleaned. The escaped Silicone Oil, if any, may cause erratic breakdown of the gas. Valves SC_4 and SC_5 allowed the gas reservoir to be connected or disconnected from the system which aided in the pressure adjustment of the gas inside the test cell. The leveler tube L_1 was raised or lowered to adjust in the cell to the desired level. After this pressure adjustment, valves SC_8 and SC_2 were closed. Also valves SC_3 and SC_4 were closed which would prevent any escape of gas while the test cell was taken out of the system. The high temperature valve SC_8 was permanently connected to the cell. The cell was then put in the oven for heating and testing.

The desired level of pressure at which the gas was filled in the test cell can be calculated as given in Appendix V. This pressure adjustment would fill the test cell with the same number of moles if the pressure and temperature was 28.35" of Hg. and 80°F, respectively.

D. Heating of the Test Cell

After filling the test cell with the gas at proper pressure, the cell was placed in the oven for heating to the desired final temperature. The lower electrode terminal of the test cell was connected to the ground terminal provided for this purpose inside the oven through a porthole. The upper electrode terminal of the cell was connected to the incoming high voltage terminal inside the oven.

The heating element control was set on high setting and the temperature indicator of the oven was set on the desired final temperature. The oven controls the set temperature automatically. The test cell was heated for about 80 minutes before conducting the impulse voltage test. The heating time of the cell was arrived after running certain heat run tests as given in Appendix VII.

The temperature of the test cell was monitored by three thermocouples number 6, 7 and 8, placed near the test cell. The thermocouples location and the method of measurement of temperature is given in Appendix VII.

E. Method of Conducting Impulse Voltage Tests

After the test cell had been heated for a proper length of time, the impulse voltage test was conducted. The impulse voltage tests were made, in general, according to the method prescribed in the ASTM Standards-Electrical Insulating Materials (Part 29, February, 1969),[18] American Standard for Measurement of Voltage in Dielectric Tests,[17] and also as recommended by M. L. Manning[6] in his paper.

The impulse voltage was started at a level that caused breakdown of the gas on less than 10 percent of the trials. Ten positive polarity $1\frac{1}{2} \times 40\ \mu$sec. pulses were applied on each voltage level with 30 seconds rest between the applications. The breakdown or no breakdown of the test gas was observed on the oscilloscope. The voltage level was then increased by 0.5 units of the panel meter. After a rest of 5 minutes, 10 pulses were applied to the test cell. This process was repeated until a level was reached where the breakdown occurred on more than 90 percent of the trials. This completed the first set of trials. The cell was dormant for 5 minutes, after which pulses of the same voltage level were applied in the similar way and the breakdowns were recorded. The voltage level was then decreased by 0.5 units of the panel meter and again 10 pulses were applied. This process was repeated until a level was reached at which breakdown occurred in less than 10 percent of the trials. Then, a repeat of the first set of trials was made. Essentially, at one voltage level, 30 pulses were applied. A sample of the test data recording is shown in Fig. 7. Then, the oven was switched off and the oven door was opened. This allowed the test cell to cool. The high voltage and the ground terminals were disconnected from the cell and the cell was taken out and it was disassembled again. The complete cycle of cleaning and filling was repeated.

The waveshape observed on the oscilloscope, when the gas flashed over and when it did not discharge are shown in Fig. 8. Test data in kilovolts was determined by using the oscilloscope calibration curve as

Date.....Dec.18th,'71 Time.....14.30.....

Type of Cell.....Sphere to Plane Electrodes Irradiation Source.....None.

Test Gap Spacing... 0.1" Final Temp. = 100.0°C

Room Pr. = 28.18"of Hg Pr. Correction....15.8"of Si.Oil

Room Temp. = 70.0°F Gap Correction....5.7mils

Oven Starting Time.....15.20 min.

Impulse Tests Starting Time....16.40 min.

Type of Wave Shape.....1½x40μ sec. Positive Polarity

Panel Meter Setting	Trials
	cycle no. 1
7.0	0 0 0 0 0 0 0 0 X 0
7.5	0 0 0 0 X X 0 0 0 0
8.0	0 0 X X X X 0 0 0 0
8.5	X X X X X 0 X X 0 0
9.0	X X X X 0 X X X X X
	cycle no. 2
9.0	X X X X X X X X X X
8.5	X X 0 X X 0 0 0 X X
8.0	0 0 0 X 0 X X X X 0
7.5	X 0 0 0 0 0 0 0 0 0
	cycle no. 3
7.5	0 0 0 0 0 0 0 0 0 0
8.0	0 0 0 X X X 0 0 0 0
8.5	X X X X X 0 0 0 0 X
9.0	X X X X X X X X X X

0=no breakdown
X= breakdown

Final Temp.101.1°C.

Fig.7 . Method of Recording the Test Datas.

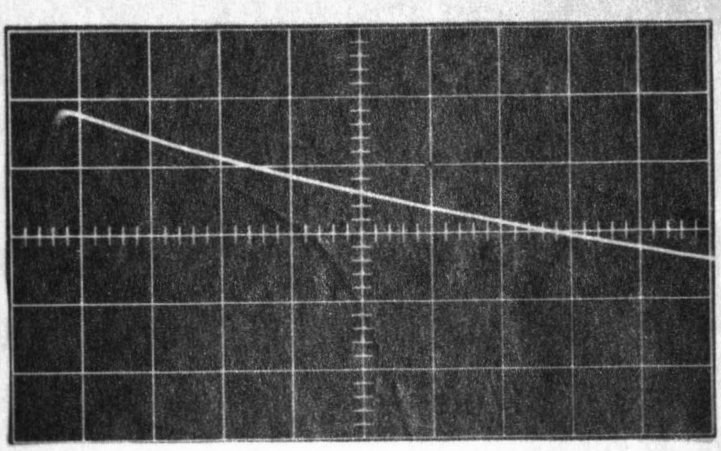

Fig. 8(a). Impulse Waveshape when no breakdown occurs.

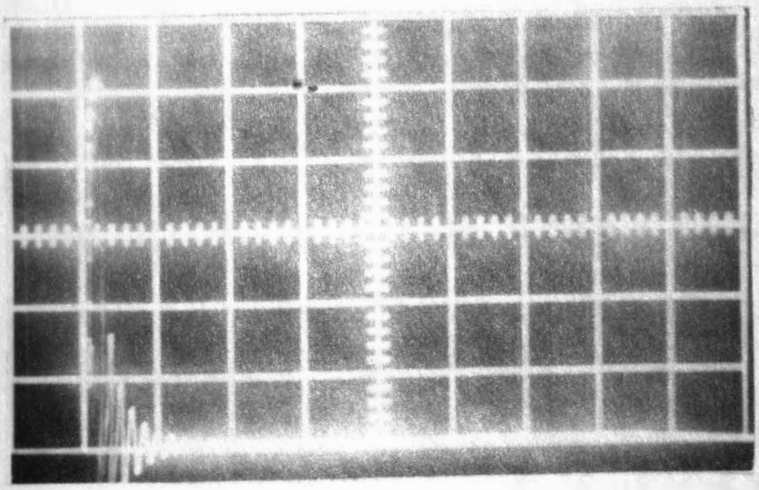

Fig. 8(b). Impulse Waveshape when the gas breaks down.

given in Appendix IV. The results of the tests are shown in Tables I through VIII of Appendix I.

CHAPTER VI

DISCUSSION OF RESULTS

A. General Description of Tables

Appendix I contains Table I through VIII. Appendix II contains Figures 10 through 18. Tables I through IV give the results of all the impulse voltage breakdown tests made on the C_3F_8 gas. The 10 percent, 50 percent and 90 percent breakdown values are listed for the gas temperature range for 25°C to 150°C. The 10 percent, 50 percent and 90 percent breakdown value for each temperature was found by plotting Applied Voltage against Percentage Breakdown. As mentioned in the Test Procedure, at each test voltage level, 30 pulses were applied. The percentage breakdown value at each voltage value was found by dividing the number of times the breakdown occurred by the total number of pulses applied. The panel meter reading was converted into the actual applied voltage by using the generator voltage calibration curve (Oscilloscope Deflection Method) as given in Appendix IV. A sample plot for finding the various percentage values of Breakdown Voltage is shown in Fig. 9. The breakdown voltage of the gas is defined as the voltage level at which the breakdown of the gas occurs 50 percent of the time. The 10 percent and 90 percent Breakdown Values are also listed to give an idea of the scattering of the results. The Range, which is the difference of 90 percent and 10 percent Breakdown Values, is also listed. Figures 10 and 11 are the plots of impulse breakdown voltage vs. gas

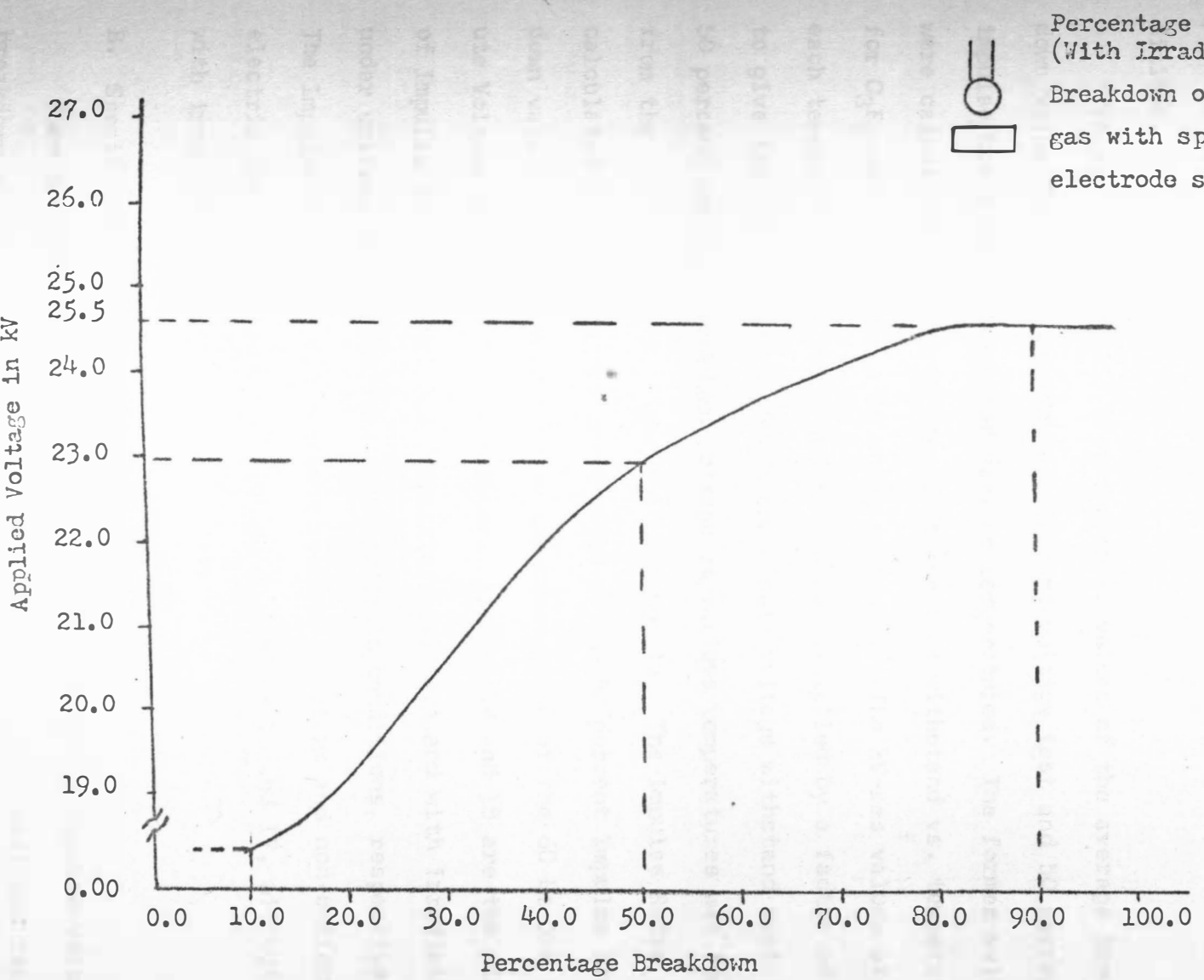

Fig.9 Method for determining 50% Breakdown Value.

temperature (under uniform and non-uniform field conditions), without and with a source of irradiation, respectively. The impulse voltage breakdown vs. gas temperature (without and with irradiation source) is plotted on Figures 12 and 13 under uniform and non-uniform field conditions.

Tables V through VIII list the crest values of the average breakdown value for 60 Hz one minute withstand voltage test and 50 percent impulse breakdown voltage for various temperatures. The former values were calculated from 60 Hz one minute voltage withstand vs. temperature for C_3F_8 gas curves given in Roman's thesis.[8] The kV-rms values at each temperature were found and they were multiplied by a factor of $\sqrt{2}$ to give the crest value of 60 Hz one minute voltage withstand test. The 50 percent impulse breakdown voltage at various temperatures was found from the curves given in Figures 10 through 13. The Impulse Ratio was calculated by dividing the crest value of the 50 percent Impulse Breakdown value at each temperature by the crest value of the 60 Hz One Minute Voltage Withstand Test breakdown. Figures 14 and 15 are the plots of Impulse Ratio against Gas Temperature (without and with irradiation) under uniform and non-uniform electric field conditions, respectively. The Impulse Ratio vs. Gas Temperature (under uniform and non-uniform electric field conditions) is plotted on Figures 16 and 17, without and with irradiation, conditions respectively.

B. Specific Observations

Some specific observations are made regarding the impulse voltage breakdown strength, 60 Hz one minute voltage withstand test and rapidly

applied voltage test, conducted on C_3F_8 gas up to 150°C. The sphere to plane electrode system would give a highly uniform field whereas the other cell used, with point to plane electrode system, would give a highly non-uniform field.

1. The impulse voltage breakdown strength of the gas under uniform field conditions is about 60 percent greater compared with non-uniform electric field conditions when no irradiation source was used. However, in the presence of an irradiation source, the strength under uniform field conditions is roughly 50 percent greater compared with non-uniform field conditions. The above statements are true for the entire range of temperatures tested (Figures 10 and 11).

2. The increase in the impulse breakdown strength of the gas as the temperature is increased is so small that for all practical purposes it can be assumed that the impulse breakdown strength of the gas remains constant throughout the range of temperature for which the gas was tested. The above statement is true for both uniform and non-uniform electric field conditions, with or without irradiation (Figures 10 and 12).

3. The impulse breakdown strength of the gas under a uniform field without irradiation is about 8 percent greater than with irradiation at 25°C gas temperature. However, as the gas temperature increases, the difference reduces progressively. At 150°C the difference is about 5 percent (Figure 12).

4. The impulse breakdown strength of the gas under non-uniform field conditions without irradiation is about 8 percent greater than

with irradiation at room temperature. As the temperature of the gas increases, the difference becomes progressively less. From 100°C and up to 150°C, the breakdown strength is the same with or without irradiation (Figure 13).

5. Under a uniform field condition, the impulse breakdown points have more scattering than under a non-uniform field condition. In other words, the breakdown point is sharper under non-uniform field conditions than under uniform field conditions. The above observation was made from Percentage Breakdown vs. Applied Voltage curves (Tables 1 through 8).

6. Also, the source of irradiation was found to reduce the scattering of the breakdown points. The temperature of the gas also affected the variation of the breakdown points slightly. At higher temperatures, less scattering was observed than at lower temperatures (Tables 2, 4, 6 and 8).

7. The Impulse Ratio of the gas under uniform field conditions increases with temperature, with and without irradiation conditions. Without irradiation, the Impulse Ratio at 150°C was found to be 10 percent greater than its value at 25°C. The corresponding figure for an irradiation condition is about 2 percent (Figure 16).

8. The Impulse Ratio of the gas under non-uniform field conditions decreases as the temperature of the gas is increased. The rate of decrease was found to be more without irradiation than with irradiation. With irradiation, the Impulse Ratio at 150°C dropped to 20 percent of

its value at room temperature. Without irradiation, the corresponding figure is 6 percent (Figure 17).

9. The Impulse Ratio of the gas under uniform field conditions at room temperature was slightly greater with irradiation than without irradiation. However, at 50°C it was the same under both the conditions. At temperatures higher than 50°C, the ratio was greater without irradiation than with irradiation (Figure 16).

10. The Impulse Ratio of the gas under non-uniform conditions at room temperature, without irradiation, was about 10 percent greater with radiation. At about 120°C, the ratio is the same with or without an irradiation condition. At 150°C, the ratio with irradiation is slightly greater than without irradiation (Figure 17).

C. Comparison-Impulse Voltage Breakdown Tests and 60 Hz Voltage Breakdown Tests Results

Roman[8] gave results of 60 Hz one minute voltage withstand tests and rapidly applied tests on C_3F_8 gas. The Impulse Ratio plots essentially show the 60 Hz one minute voltage withstand as compared with the impulse voltage breakdown strength. Following are some of the observations made in comparing the results of 60 Hz rapidly applied voltage breakdown tests and impulse voltage breakdown tests.

1. Unlike impulse voltage breakdown strength, the 60 Hz rapidly applied voltage breakdown strength decreases with the increase in the gas temperature under uniform field conditions for with and without irradiation conditions.

2. The rapidly applied voltage breakdown strength of the gas under non-uniform field conditions, increases with temperature whereas it decreases or remains constant for impulse voltage tests.

D. Observations Linked with Theory

The experimental results obtained are analyzed in light of the theory of electric discharges through the gases. It should be recalled that C_3F_8 belongs to the electronegative group of gases. The electrons which eventually lead to the breakdown of the gas are produced due to one or more of the following mechanisms: (1) photo-ionization and secondary ionization, (2) ionization due to presence of source of irradiation, (3) thermal ionization and, (4) a non-uniform field. The majority of these electrons are given off at the cathode. The basic theory of the electric discharges through the gases and mechanism of spark breakdown is given in Chapter III.

The gas takes a certain time to breakdown completely after the application of necessary voltage. This time lag between the application of the voltage and the breakdown can be divided into two parts. The statistical time lag is the average time required for a primary electron to appear in the gap after the application of voltage which is capable of leading to the breakdown. The formation time lag is the time taken by the gas to breakdown completely after the appearance of primary electrons in the gap if sufficient voltage was applied. The statistical time lag depends upon the number of primary electrons released from the cathode or produced in the gap. This in turn depends on irradiation conditions and thermal ionization. The formative lag is

dependent upon the transit time taken by a positive ion from anode to cathode. The scattering or the variation of breakdown strength in fact gives an idea of the variation of the time lag.

The uniform field produces fewer electrons as compared with the non-uniform field. Consequently, the statistical time lag under uniform field conditions would be larger than under non-uniform field conditions. Since few electrons are produced under uniform field conditions, the probability of the variation of the statistical time lag is high. However, in case of non-uniform field conditions, the reverse would be true. The statistical time would be reduced if the source of irradiation is present and also by the thermal ionization if the temperature of the gas is high. In the curves of Percentage Breakdown vs. Applied Voltage, the author found that uniform field impulse breakdown, in general, had more scattering than the impulse breakdown under non-uniform field conditions. The presence of source of irradiation also reduces the scattering for both types of electrode systems. Also, the scattering was slightly lower at higher temperatures than for lower temperatures. These observations, in general, showed substantial agreement with the theroy. However, other processes are also involved which effect the scattering of the results such as negatively ion space charges and the formation of positive ions in the gap.

In electronegative gases like C_3F_8, strong electric fields would cause the formation of ion sheath formed by positive ions. The positive ions are formed as a result of the C_3F_8 gas loosing fluoro ions instead

of electrons. The positive ion sheath thus formed would prevent the conduction, thereby increasing the breakdown strength.

The production of primary electrons in the uniform field is lower than in the non-uniform field. This reduces the breakdown strength of the gas under non-uniform field conditions as compared with uniform electric field conditions due to the increased availability of the number of free electrons. The effect of negative ion space charge, and/or the formation of heavy positive ions in case of non-uniform fields apparently is not large enough to upset the above effect for the temperatures up to 150°C.

The effect of high temperature would be increased ionization of the gas. This would tend to decrease the breakdown strength of the gas. However, the effect was very insignificant for test temperatures up to 150°C. For all practical purposes, breakdown voltages more or less remained constant with increase in temperature. The above holds good for both types of electric fields. The presence of source of irradiation would increase the production of primary electrons for the eventual breakdown. The increased availability of primary electrons would tend to reduce the breakdown strength of the gas. As the temperature increases, the effect of primary electrons due to source of irradiation would be less pronounced due to increased thermal ionization. The source of irradiation would also cause to increase the number of free electrons. This would increase the number of primary electrons available for attachment to form negative ions and the space charge effect would be more

pronounced. This factor contributes in the increase of the breakdown strength of the gas. Also, the increase in the number of primary electrons available for conduction would decrease the breakdown strength of the gas. Both the effects are directed against each other and the net effect observed was a decrease in the breakdown strength of the gas in presence of an irradiation source. At higher temperatures, thermal ionization produces enough electrons so that the effect of irradiation is hidden. This was especially found to be true under non-uniform electric field conditions.

CHAPTER VII

CONCLUSIONS

The following conclusions apply to C_3F_8 gas tested for temperature range of 25°C to 150°C.

1. The impulse voltage breakdown strength of the gas under uniform field conditions is higher compared with non-uniform field conditions. This is true with or without irradiation.

2. The impulse breakdown voltage strength of the gas increases slightly, or remains constant, as the temperature of the gas in increased. This holds true regardless of non-uniform or uniform electric field conditions, with or without irradiation.

3. The impulse voltage breakdown strength of the gas under uniform electric field conditions is about 5 percent greater without irradiation conditions than with irradiation. This is true at any temperature.

4. The impulse voltage breakdown strength of the gas under non-uniform electric field conditions is greater up to 100°C temperatures without irradiation as compared with irradiation. However, above 100°C temperatures it is the same.

5. The breakdown points have less variation with non-uniform field as compared with uniform electric field conditions. The presence of a source of irradiation also reduces the variation. Higher temperature of the gas reduces the variation slightly.

6. The variation of the impulse voltage breakdown strength with temperature is due to the effect of thermal ionization.

7. Without irradiation, the Impulse Ratio of the gas under uniform electric field conditions increases as the temperature of the gas increases.

8. Without irradiation, the Impulse Ratio rate of increase under uniform electric field conditions is greater compared with radiation exposure.

9. With irradiation, the Impulse Ratio of the gas under non-uniform electric field conditions decreases slightly as the temperature of the gas increases. The variation is less with irradiation. Without irradiation, the Impulse Ratio of the gas under non-uniform electric field conditions decreases more rapidly compared with irradiation.

10. The Impulse Ratio of the gas is greater under uniform electric field conditions than under non-uniform electric field conditions and this ratio depends upon the gas temperature. It is less with irradiation at any temperature. This is true for with or without irradiation.

11. The Impulse Ratio of the gas under uniform electric field conditions is slightly greater at lower temperatures with irradiation as compared without irradiation.

12. With irradiation, the Impulse Ratio of the gas under non-uniform electric field conditions is lower at lower temperatures. At higher temperatures beginning at 125°C, the Impulse Ratios are similar. Without irradiation, the Impulse Ratio is greater at lower temperatures and decreases quite markedly as the temperature is increased to 150°C.

LITERATURE CITED

1. M.L.Manning and E.D.Padgett, "Gaseous Dielectric Materials - Applications and Test Methods," Electrical Manufacturing, (October, 1958) pp. 86-90.

2. G.Camilli and J.J.Chapman, " Gaseous Insulation for High Voltage Apparatus," AIEE Transactions,Vol.66,1947,pp. 1463-1470.

3. G.Camilli and R.E.Plump, "Fluorine Containing Gaseous Dielectrics," AIEE Transactions,Vol.72,1953,pt.1,pp. 93-102.

4. C.N.Works and T.W.Dakin, "Dielectric Breakdown of SF_6 in Non-Uniform Fields," AIEE Transactions,Vol.72,1953,pt.1,pp. 682-687.

5. Product Data Sheet #PD-TA-218-4-58, Product Development Department, General Chemical Division, Allied Chemical Corporation.

6. M.L.Manning, "Experience with the AIEE Subcommittee Test Cell for Gaseous Insulation," AIEE Paper 59-114 Winter General Meeting, New York,N.Y.,(Febuary, 1959).

7. L.C.Whitman, "Impulse Voltage Tests on Air and C_3F_8 ," IEEE Conference Paper 65-62 Winter Power Meeting, New York,N.Y., (January, 1965).

8. E.J.Roman, "Voltage Breakdown Strength vs. Temperature of Octafluoropropane Gas Exposed to Uniform and Non-Uniform Electric Fields,"South Dakota State University,Brookings,South Dakota, Thesis,(Janruary, 1970).

9. L.L.Alston, "High Temperature Effects on Flashover in Air," IEE Proceedings,Vol. 105,1958,pp. 549-553.

10. A.H.Sharbaugh,P.K.Watson,D.R.White,T.H.Lee and A.Greenwood, "An Investigation of the Breakdown Strength of Nitrogen at High Temperatures Using a Shock Tube," AIEE Paper 61-136 Winter General Meeting,New York,N.Y.,(January, 1961).

11. A.M.Howatson, An Introduction to Gas Discharges, Oxford: Peragamon Press, (1961) pp. 42-78.

12. L.B.Loeb, Fundamental Processes of Electrical Discharge in Gases: John Wiley and Sons,(1939) pp. 86-484.

13. J.M.Meeks and J.D.Craggs, Electrical Breakdown of Gases,Oxford Press,(1953) pp. 251-289.

14. L.L.Alston, "The Impulse Initiation of Arc Discharges," IEE Proceedings,Vol. 105, 1958, pp. 133-140.

15. T.J.Lanoue, "The Effect of Test Cell Glass Cylinder Diameter on Gaseous Insulation Dielectric Strength," South Dakota State University,Brookings,South Dakota,Thesis,(1968).

16. Keith E.Crouch, "The Effect of Wave Shape on the Electrical Breakdown of Nitrogen Gas," South Dakota State University, Brookings,South Dakota,Thesis,(June, 1966).

17. American Standard for Measurement of Voltage in Dielectric Tests, AIEE Standard 4, A.S.A. c68.1, (1953).

18. ASTM Standards, Part 29, Easton,Maryland: American Society for Testing and Materials, (Febuary, 1969) pp. 1154-1164.

19. L.L.Alston, High Voltage Technology: Oxford University Press, (1968),pp. 17-44.

20. P.R.Howard, "Insulation Properties of Compressed Electronegative Gases," IEE Proceedings,Vol. 104 (1957), pp. 123-137.

APPENDIX I

TABLE I

Impulse Voltage Breakdown Strength of C_3F_8 gas for the Sphere to Grounded Plane Electrode System at Various Gas Temperatures, without a Source of Irradiation.

Type of Wave: $1\frac{1}{2} \times 40 \mu$sec. Positive Polarity

Various Values of Breakdown Voltages from ten trials	Gas Temperature in °C					
	27.5	48.0	74.8	101.8	126.0	146.8
10% Breakdown Value (kV)	25.20	24.25	25.20	24.50	24.10	26.10
50% Breakdown Value (kV)	27.04	26.60	26.98	26.56	26.80	27.50
90% Breakdown Value (kV)	27.77	28.20	28.05	27.45	27.63	28.45
Range (kV)	2.57	3.95	2.85	2.95	3.53	2.35

TABLE II

Impulse Voltage Breakdown Strength of C_3F_8 gas for the Sphere to Grounded Plane Electrode System at Various Gas Temperatures, with a Source of Irradiation.

Type of Wave: $1\frac{1}{2} \times 40 \mu$sec. Positive Polarity

Various Values of Breakdown Voltages from ten trials	Gas Temperature in ^{o}C					
	28.0	46.7	71.1	101.2	121.5	144.1
10% Breakdown Value (kV)	22.10	23.90	22.20	23.45	23.30	23.35
50% Breakdown Value (kV)	24.07	25.57	24.46	25.52.	24.03	25.20
90% Breakdown Value (kV)	26.17	26.75	26.20	26.65	24.95	26.75
Range (kV)	4.07	2.85	4.00	2.80	1.65	3.40

TABLE III

Impulse Voltage Breakdown Strength of C_3F_8 gas for the Point to Grounded Plane Electrode System at Various Gas Temperatures, without a Source of Irradiation.
Type of Wave: $1\frac{1}{2} \times 40 \mu$sec. Positive Polarity

Various Values of Breakdown Voltages from ten trials	Gas Temperature in ^{o}C					
	31.6	53.3	69.3	100.0	128.5	146.2
10% Breakdown Value (kV)	15.85	15.85	16.10	14.60	16.30	14.35
50% Breakdown Value (kV)	16.76	16.80	17.72	15.61	16.83	15.70
90% Breakdown Value (kV)	17.34	17.50	18.28	16.25	17.50	16.68
Range (kV)	1.49	1.65	2.18	1.65	1.20	2.33

TABLE IV

Impulse Voltage Breakdown Strength of C_3F_8 gas for the Point to Grounded Plane Electrode System at Various Gas Temperatures, with a Source of Irradiation.
Type of Wave: $1\frac{1}{2} \times 40 \mu$sec. Positive Polarity

Various Values of Breakdown Voltages from ten trials	Gas Temperature in °C					
	23.5	51.2	75.8	101.1	126.5	148.6
10% Breakdown Value (kV)	15.17	16.40	16.40	16.40	16.30	16.55
50% Breakdown Value (kV)	15.88	17.20	17.28	16.76	16.86	16.84
90% Breakdown Value (kV)	16.75	17.56	17.57	17.05	17.12	17.20
Range (kV)	1.58	1.16	1.17	0.65	0.82	0.65

TABLE V

Impulse Ratios of C_3F_8 gas at Various Gas Temperatures for the Sphere to Grounded Plane Electrode System, without Irradiation. Type of Wave: $1\frac{1}{2} \times 40 \mu$ sec. Positive Polarity

Various Values of Breakdown Voltages and Impulse Ratio	Gas Temperature in °C					
	25.0	50.0	75.0	100.0	125.0	150.0
Crest Value of Average Breakdown Value for 60 Hz One Minute Withstand Voltage Tests in kV	23.5	22.9	22.0	21.7	21.5	21.2
50% Breakdown Value for Impulse Voltage Tests in kV	27.1	26.6	26.4	26.4	26.6	27.2
Impulse Ratio	1.15	1.16	1.20	1.21	1.23	1.28

TABLE VI

Impulse Ratios of C_3F_8 gas at Various Gas Temperatures for the Sphere to Grounded Plane Electrode System, with Irradiation.
Type of Wave: $1\frac{1}{2} \times 40 \mu$sec. Positive Polarity

Various Values of Breakdown Voltages and Impulse Ratio	Gas Temperature in °C					
	25.0	50.0	75.0	100.0	125.0	150.0
Crest Value of Average Breakdown Value for 60 Hz One Minute Withstand Voltage Tests in kV	21.2	21.2	21.2	21.2	21.2	21.2
50% Breakdown Value for Impulse Voltage Tests in kV	24.8	24.7	24.6	24.8	25.0	25.5
Impulse Ratio	1.17	1.165	1.16	1.17	1.18	1.20

TABLE VII

Impulse Ratios of C_3F_8 gas at Various Gas Temperatures For the Point to Grounded Plane Electrode System, without Irradiation. Type of Wave: $1\frac{1}{2} \times 40 \mu$ sec. Positive Polarity

Various Values of Breakdown Voltages and Impulse Ratio	Gas Temperature in °C					
	25.0	50.0	75.0	100.0	125.0	150.0
Crest Value of Average Breakdown Value for 60 Hz One Minute Withstand Voltage Tests in kV	14.7	15.2	15.7	16.4	17.0	17.5
50% Breakdown Value for Impulse Voltage Tests in kV	17.2	17.2	17.0	16.9	16.7	16.8
Impulse Ratio	1.17	1.13	1.04	1.02	0.985	0.96

TABLE VIII

Impulse Ratios of C_3F_8 gas at Various Gas Temperatures for the Point to Grounded Plane Electrode System, with Irradiation.
Type of Wave: $1\frac{1}{2} \times 40 \mu$ sec. Positive Polarity

Various Values of Breakdown Voltages and Impulse Ratio	Gas Temperatures in °C					
	25.0	50.0	75.0	100.0	125.0	150.0
Crest Value of Average Breakdown Value for 60 Hz One Minute Withstand Voltage Tests in kV	15.5	15.8	16.2	16.5	16.8	17.1
50% Breakdown Value for Impulse Voltage Tests in kV	16.3	16.4	16.4	16.6	16.7	16.8
Impulse Ratio	1.05	1.03	1.01	1.005	0.995	0.980

APPENDIX II

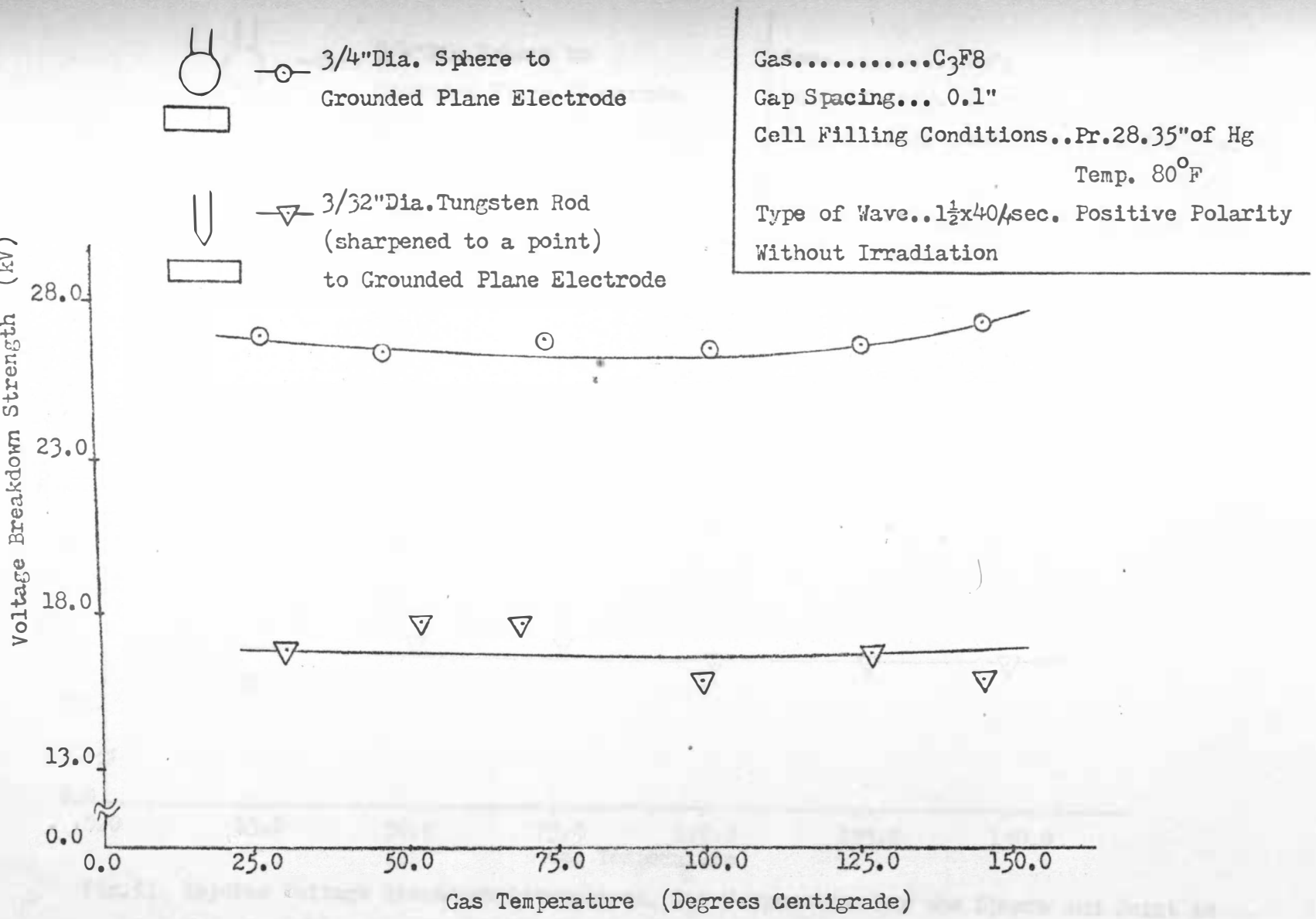

Fig.10 Impulse Voltage Breakdown Strength vs. Gas Temperature for the Sphere and Point to Grounded Plane Electrode System, without Irradiation.

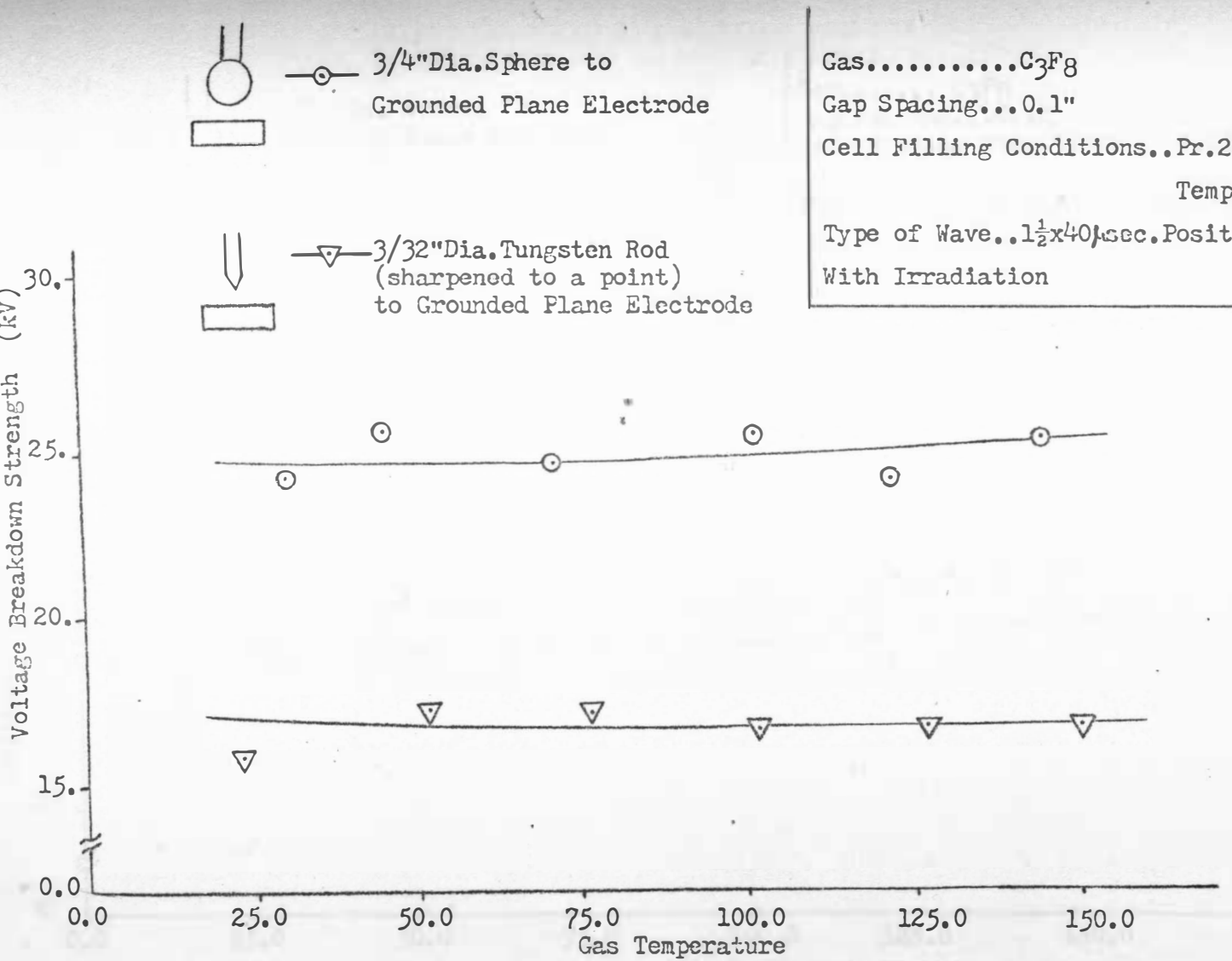

Fig.11 Impulse Voltage Breakdown Strength vs. Gas Temperature for the Sphere and Point to Grounded Plane Electrode Systems with Irradiation.

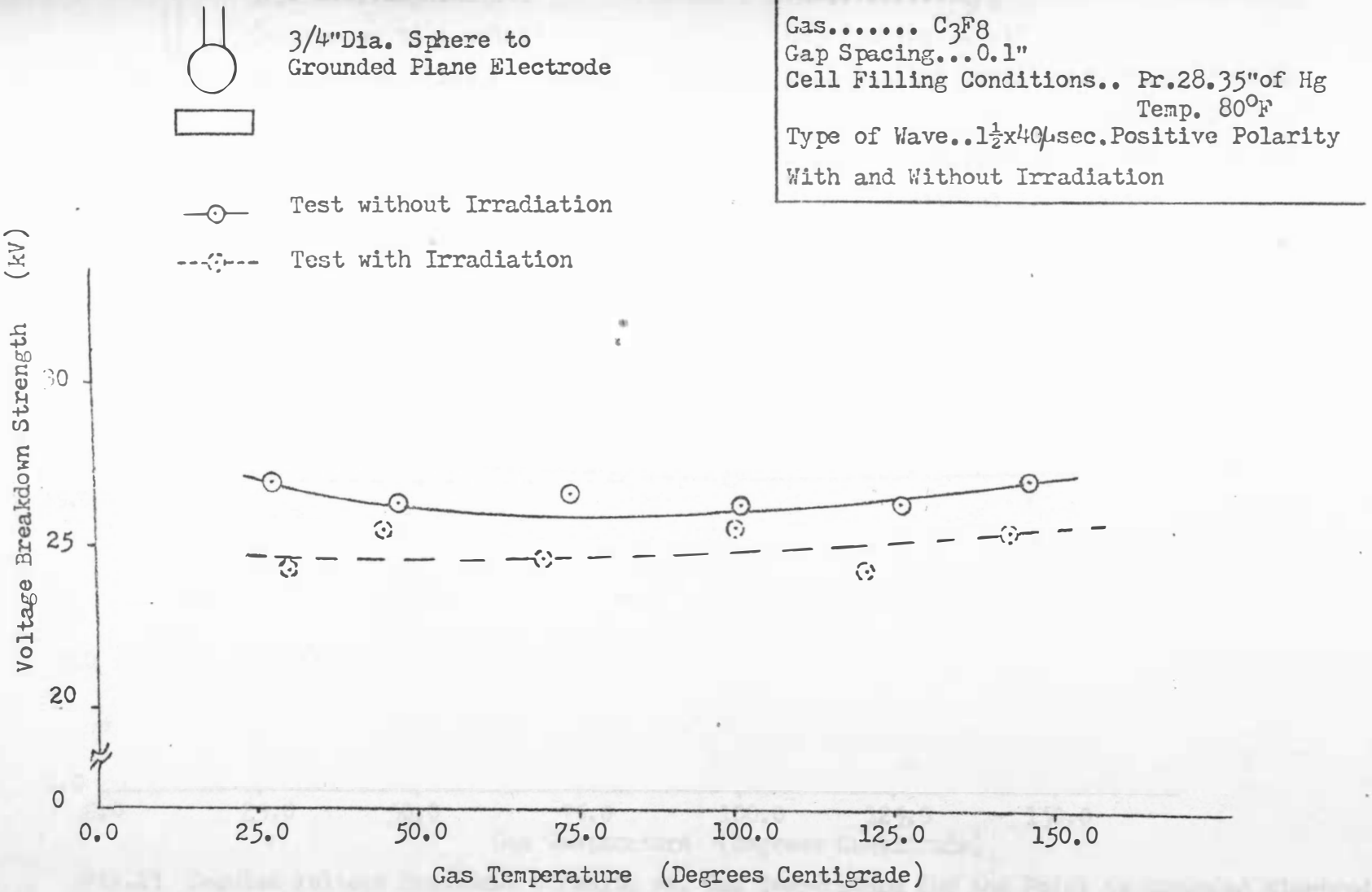

Fig.12 Impulse Voltage Breakdown Strength vs. Gas Temperature for the Sphere to Grounded Plane Electrode System, with and without source of irradiation.

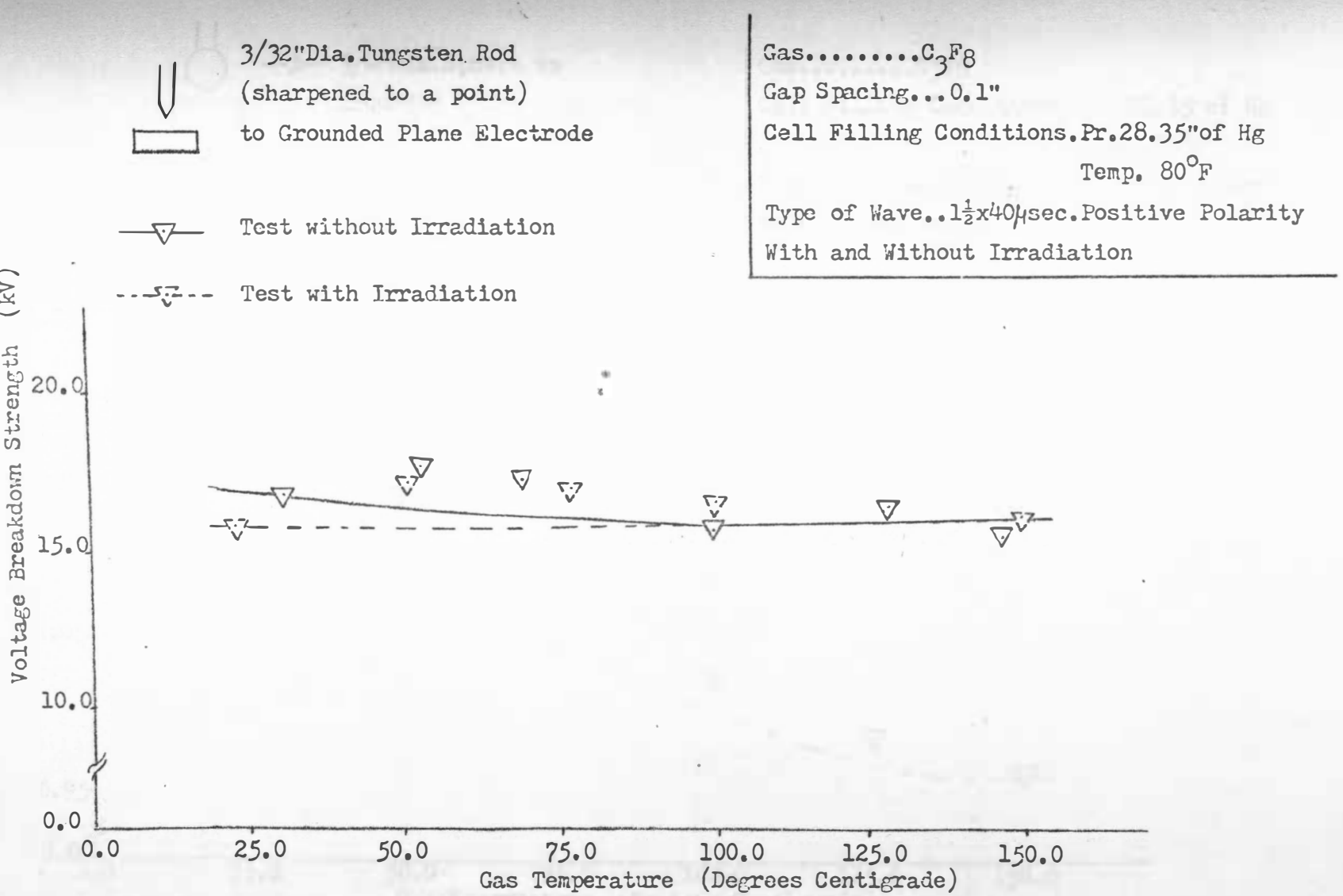

Fig.13 Impulse Voltage Breakdown Strength vs. Gas Temperature for the Point to Grounded Electrode System, with and without source of Irradiation.

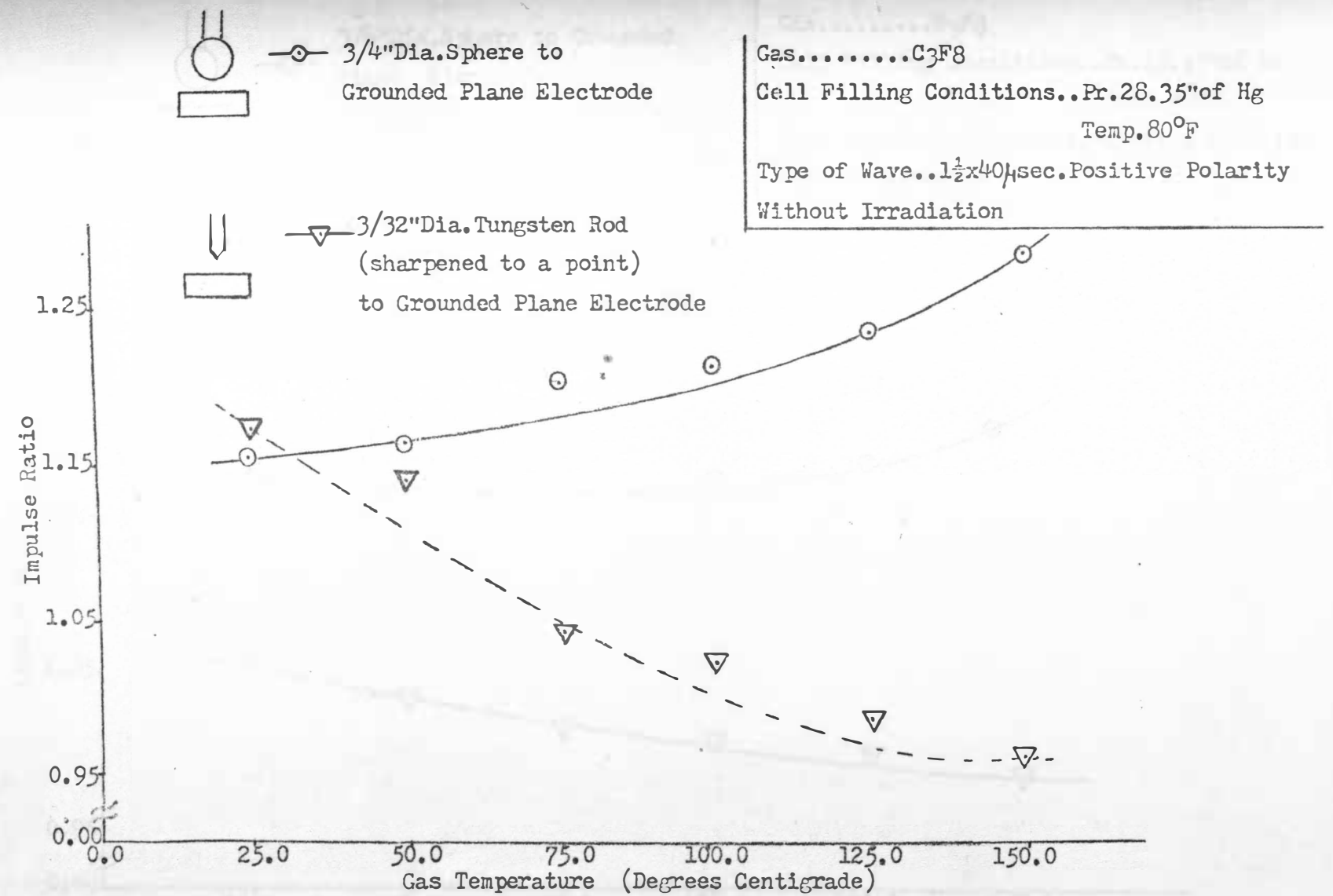

Fig.14 Impulse Ratios vs. Gas Temperature for the Sphere and Point to Grounded Plane Electrodes Systems without Irradiation.

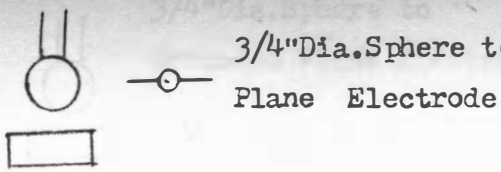

3/4"Dia.Sphere to Grounded Plane Electrode

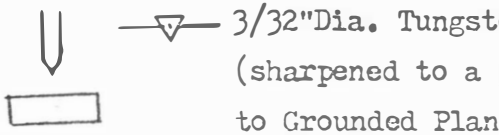

3/32"Dia. Tungsten Rod (sharpened to a point) to Grounded Plane Electrode

Gas.....C_3F_8

Cell Filling Conditions..Pr.28.35"of Hg

Temp.80°F

Type of Wave..$1\frac{1}{2}$x40μsec.Positive Polarity

With Irradiation

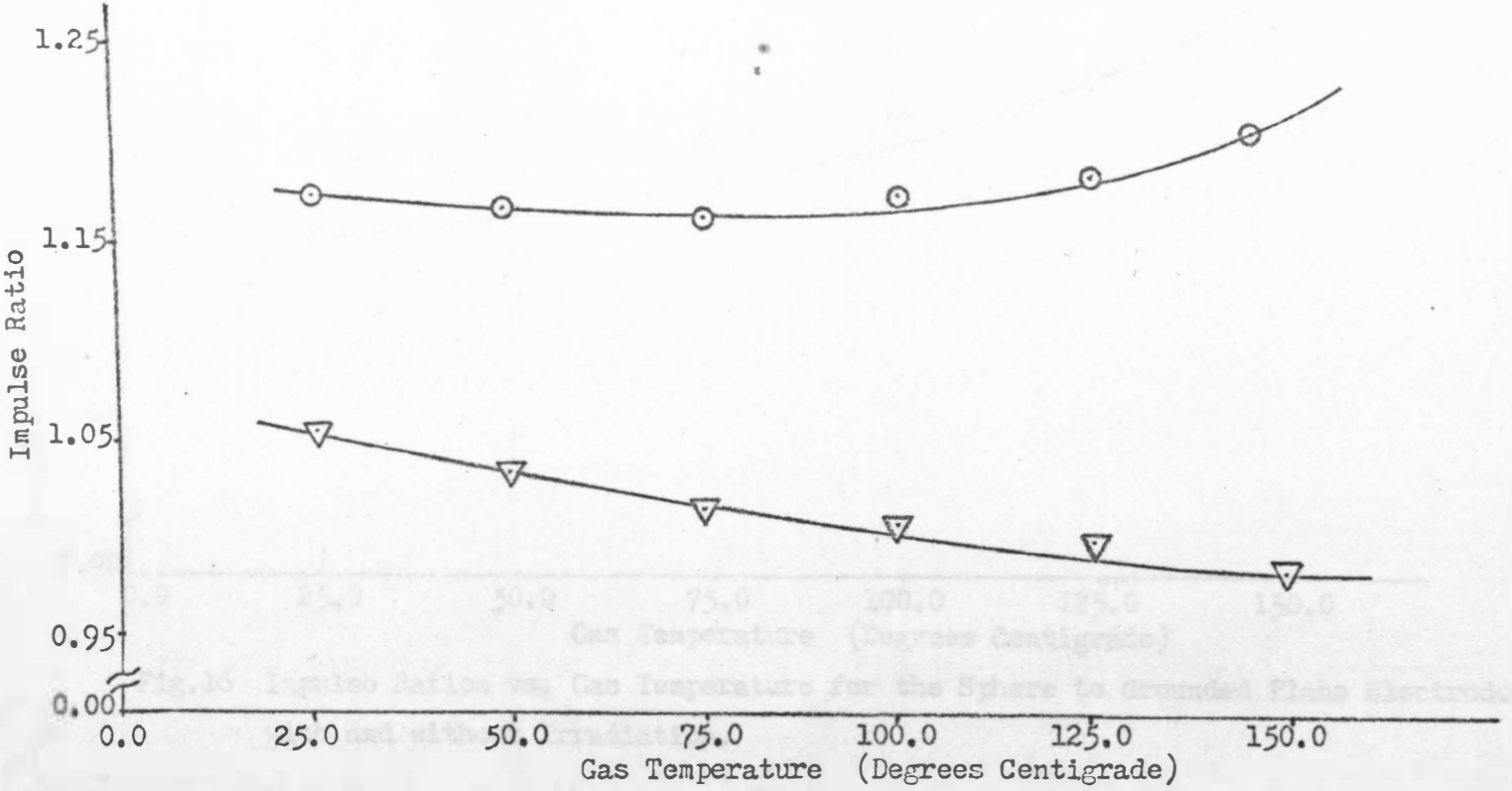

Fig.15 Impulse Ratios vs. Gas Temperature for the Sphere and Point to Grounded Plane Electrode Systems with Irradiation

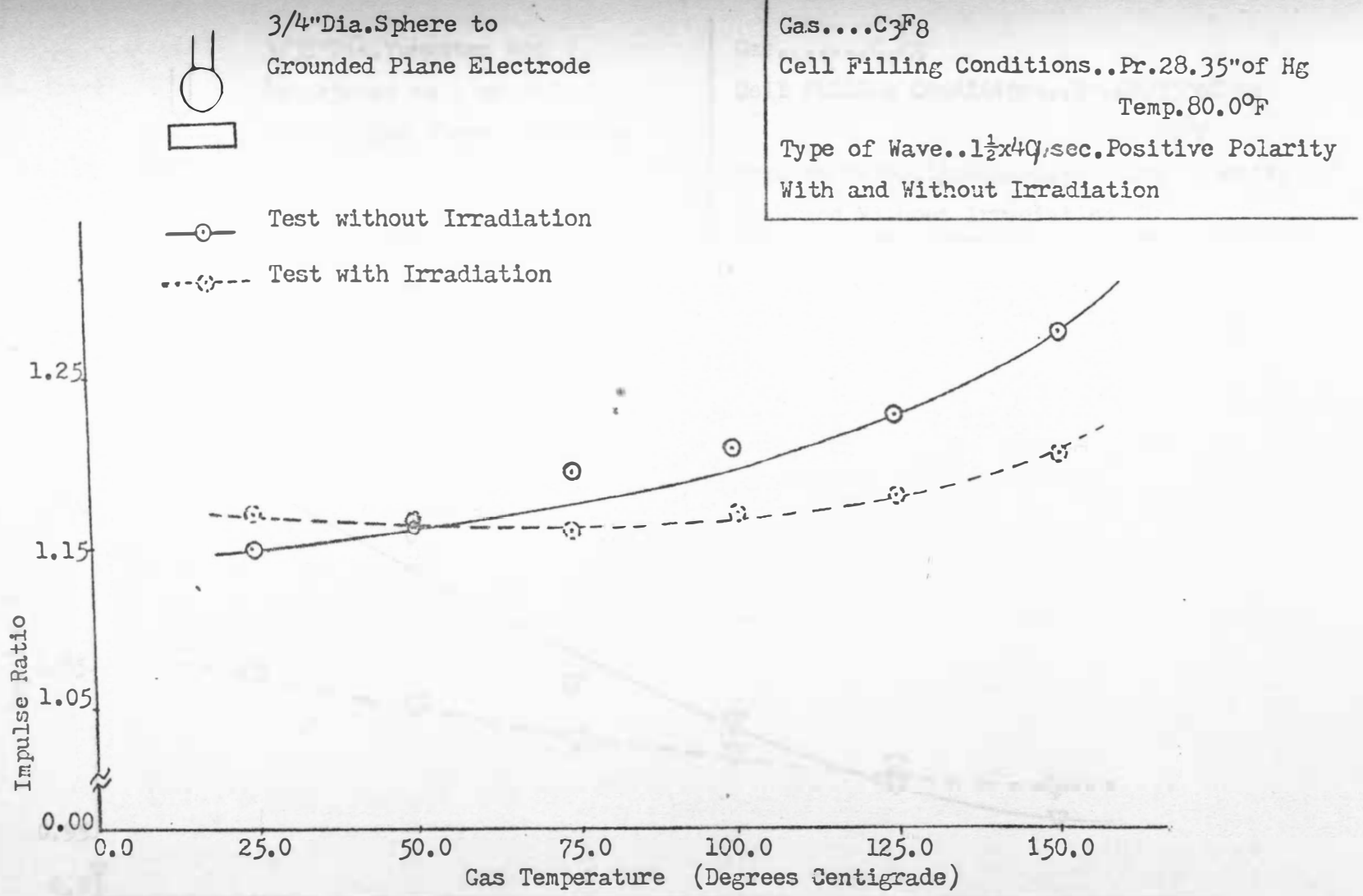

Fig.16 Impulse Ratios vs. Gas Temperature for the Sphere to Grounded Plane Electrode System, with and without Irradiation.

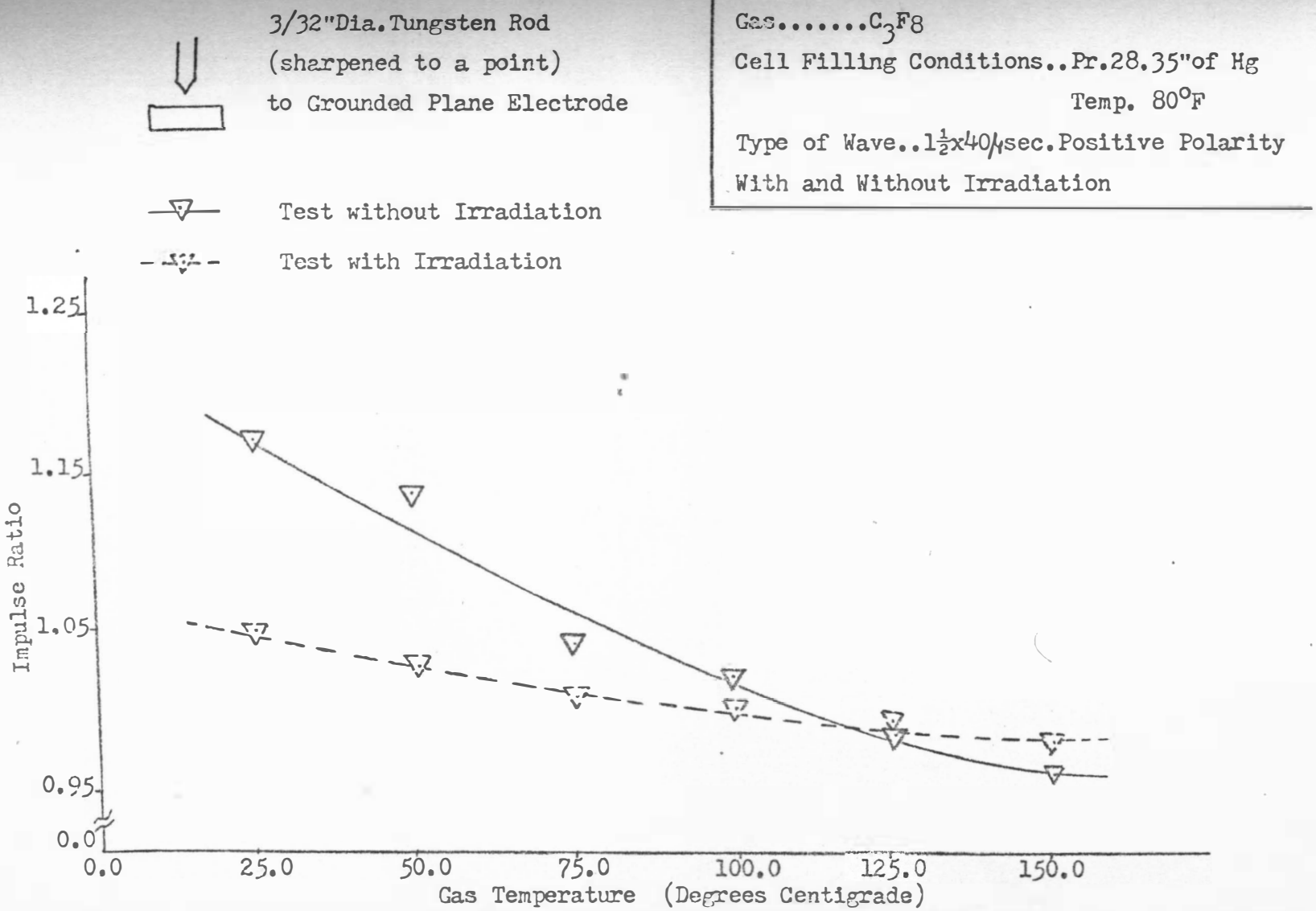

Fig.17 Impulse Ratio vs. Gas Temperature for the Point to Grounded Plane, with and without Irradiation.

APPENDIX III

DETERMINATION OF THE STANDARD IMPULSE WAVE SHAPING CIRCUIT - BY THEORY AND BY PRACTICE

A. Theory

The impulse wave shape used in the testing of electric breakdown strength of materials was that specified by AIEE Standard # 4,1953.[17] This standard waveshape is specified as a $1\frac{1}{2} \times 40$ μsec. wave which rises to its peak value in $1\frac{1}{2}$ μsec. and then decays to half of the peak value in 40 μsec. The wave recorded during a test should confirm to the specified wave within permissible tolerances as given in the Standards.

Mathematical Analysis of Waveshaping Circuit: Consider an impulse wave with peak voltage V, rise to time t_1 and time of decay to its half peak value t_2, as shown in Figure 18. The waveshaping circuit used in the testing was a RC circuit. The equivalent circuit representing the

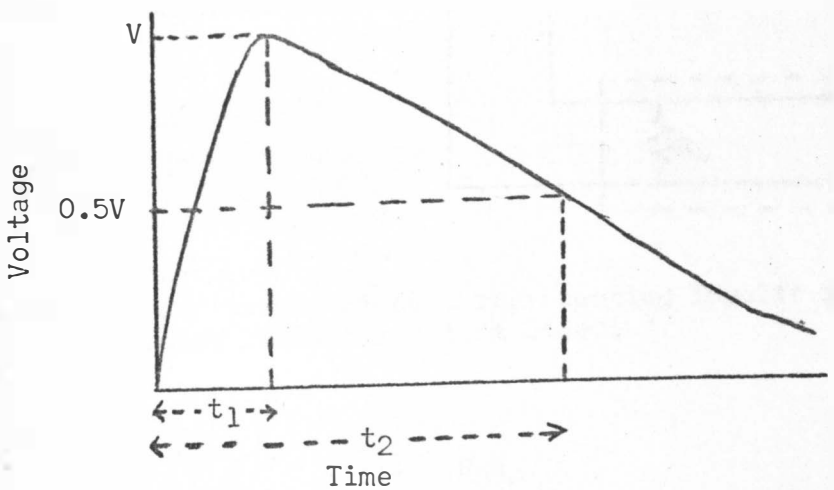

Fig. 18. Waveshape of positive polarity wave.

impulse generator, waveshaping circuit and the oscilloscope is shown in Figure 19, where C_1 is the combined capacitance of the capacitor bank in the impulse generator, V_0 is the voltage across C_1 when fully charged, R_4 is the input resistance of oscilloscope. R_1 is resistance added for wave form control, R_2 and R_3 are resistors for controlling the length of the wave. Capacitance C_2 represents the electrostatic capacitance to ground of the high voltage parts and leads. Included in C_2 is any additional load capacitance that may be required.

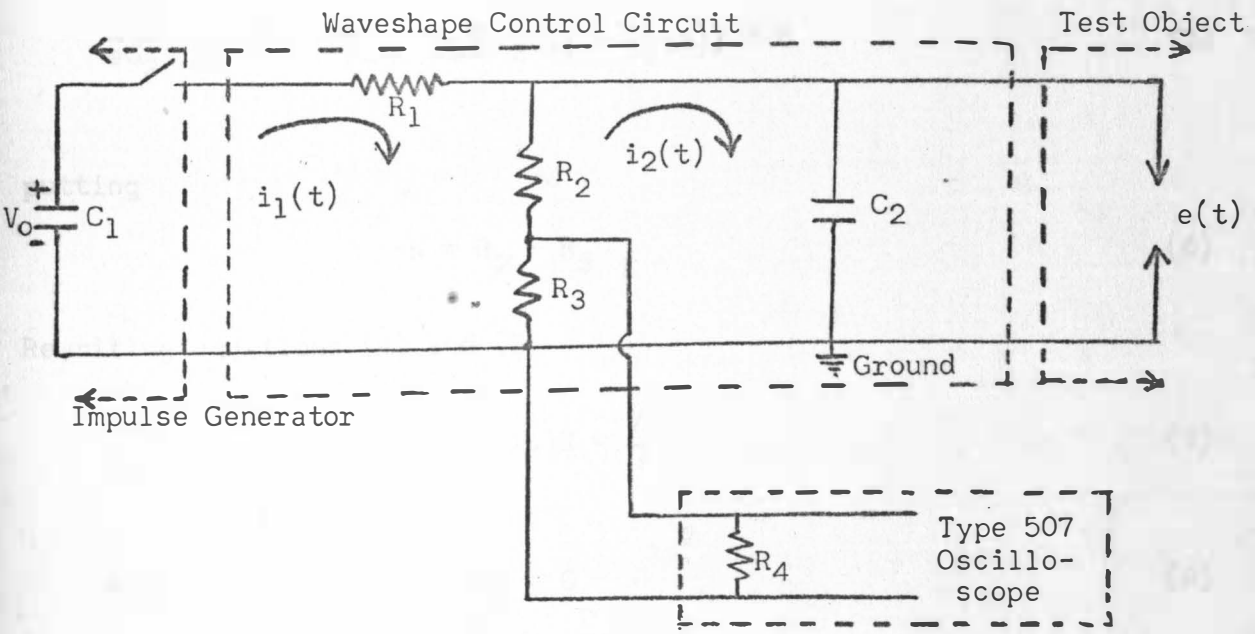

Fig. 19. An equivalent circuit representing impulse generator, waveshaping circuit and test object.

Let $$R = \frac{R_3 R_4}{R_3 + R_4} \qquad (1)$$

From Figure 19, two loop equations can be written

$$\frac{1}{C_1}\int i_1(t)dt - V_0 + R_1 i_1(t) + (R_2 + R_5)[i_1(t) - i_2(t)] = 0 \qquad (2)$$

$$\frac{1}{C_2}\int i_2(t)dt + (R_2 + R_5)[i_2(t) - i_1(t)] = 0 \qquad (3)$$

Taking Laplace Transform of equations (2) and (3)

$$\frac{1}{sC_1} I_1(s) - \frac{V_o}{s} + R_1 I_1(s) + (R_2 + R_5)[I_1(s) - I_2(s)] = 0 \qquad (4)$$

$$\frac{1}{sC_2} I_2(s) + (R_2 + R_5)[I_2(s) - I_1(s)] = 0 \qquad (5)$$

putting

$$R = R_2 + R_5 \qquad (6)$$

Rewriting equations (4) and (5)

$$I_1(s)[\frac{1}{sC_1} + R_1 + R] - I_2(s)R = \frac{V_o}{s} \qquad (7)$$

$$R\, I_1(s) + I_2(s)[\frac{1}{sC_2} + R] = 0 \qquad (8)$$

Simplifying the above equations

$$I_2(s) = \frac{1}{R}[(\frac{1}{sC_1} + R_1 + R)I_1(s) - \frac{V_o}{s}] \qquad (9)$$

$$I_1(s) = [\frac{\frac{1}{sC_2} + R}{R}] \times I_2(s) \qquad (10)$$

Substituting the value of $I_1(s)$ from equation (10) unto (9)

$$I_2(s) = \frac{1}{R}\left[\left(\frac{1}{sC_1} + R + R\right) x \frac{\frac{1}{sC_2} + R}{R} I_2(s) - \frac{V_o}{s}\right]$$

or

$$I_2(s) = \frac{sC_1C_2 R V_o}{s^2(C_1C_2 R R_1) + s(C_1R_1 + C_1R + C_2R) + 1} \qquad (11)$$

The output voltage is

$$e(t) = \frac{1}{C_2}\int i_2(t)dt$$

Taking Laplace transform of equation (12)

$$E(s) = \frac{I_2(s)}{sC_2} \qquad (13)$$

Substituting equation (11) into equation (13), then

$$E(s) = \frac{C_1RV_o}{s^2(C_1C_2 R R_1) + s(C_1R_1 + C_1R + C_2R) + 1} \qquad (14)$$

Now let

$$A = C_1C_2 R R_1 , \quad B = C_1(R_1 + R) + C_2R , \quad D = C_1RV_o$$

Equation (10) becomes

$$E(s) = \frac{D/A}{(s + \frac{B}{2A})^2 + (\frac{1}{A} - \frac{B^2}{4A^2})} \qquad (15)$$

Taking inverse Laplace transform of equation (15)

$$e(t) = D/2A\,B[e^{-(\alpha-\beta)t} - e^{-(\alpha+\beta)t}] \tag{16}$$

where

$$\alpha = \frac{B}{2} \text{ and } \beta = \frac{B}{4A^2} - \frac{1}{A}$$

Now t_1 is defined as the time for the voltage to reach the peak or maximum value. Therefore, to obtain time t_1, equation (12) is differentiated with respect to t, set equal to zero and solved for t_1.

$$\frac{de(t)}{dt} = -(\alpha-\beta)e^{-(\alpha-\beta)t} + (\alpha+\beta)e^{-(\alpha+\beta)t} \tag{17}$$

Setting $\frac{de(t)}{dt}$ equal to zero, the value of t_1 becomes

$$t_1 = \frac{\ln[(\alpha+\beta)/(\alpha-\beta)]}{2} \tag{18}$$

The value of time t_2 can be found in the following way

By definition

$$e(t_1) = 2e(t_2)$$

therefore, from equation (12)

$$\frac{D}{2A}[e^{-(\alpha-\beta)t_1} - e^{-(\alpha+\beta)t_1}] = \frac{D}{A}[e^{-(\alpha-\beta)t_2} - e^{-(\alpha+\beta)t_2}] \tag{19}$$

now $e^{-(\alpha-\beta)t_1} \gg e^{-(\alpha+\beta)t_1}$

and $e^{-(\alpha-\beta)t_2} \gg e^{-(\alpha+\beta)t_2}$

Neglecting the comparatively smaller terms, equation (15) becomes

$$e^{-(\alpha-\beta)t_1} = 2e^{-(\alpha-\beta)t_2} \tag{20}$$

Take the natural loqarthim of equation (20) and solving for t_2

$$t_2 = 0.694/(\alpha - \beta) + t_1 \tag{21}$$

The known parameters are

$t_1 = 1.5\,\mu$sec. $\qquad R_3 = 75.6$ ohms

$t_2 = 40\,\mu$sec. $\qquad R_4 = 72.8$ ohms

$C_1 = 0.05/3$ fd $\qquad A = 5.62 \times 10^{-17}\ R\ R$

$C_2 = 0.00337$ fd $\qquad B = 2.005 \times 10^{-8}\ R + 1.668 \times 10^{-8}\ R_1$

Substituting these values in equation (18) and (21), then the following relations are derived.

$$1.668R_1 + 2.005R = 0 \tag{22}$$

$$R^2 + 1.102\ R\ R_1 + 0.692R_1^2 = 0 \tag{23}$$

Solving the two equations

$R = 1550$ ohms, $R_1 = 106$ ohms

From equations (1) and (6), value of R_2 can be found

$R_2 = 1512.9$ ohms

The simplified mathematical equation of impulse wave is derived as following

Equation (14) can be rearranged as

$$E(s) = \frac{V_o}{s} \times \frac{R}{R\,R_1\,C_2 s + \frac{1}{sC_1} + \frac{R\,C_2}{C_1} + R + R_1}$$

$$= \frac{V_o}{R_1 C_2} \times \frac{1}{s^2 + (\frac{1}{R_1 C_1} + \frac{1}{RC_2} + \frac{1}{R_1 C_2})s + (\frac{1}{R_1 R\,C_1 C_2})}$$

or

$$E(s) = \frac{V_o}{R_1 C_2} \times \frac{1}{s^2 + as + b} \tag{24}$$

where

$$a = (\frac{1}{R_1 C_1} + \frac{1}{R\,C_2} + \frac{1}{R_1 C_2})$$

and

$$b = \frac{1}{R\,R_1\,C_1 C_2}$$

$$E(s) = \frac{V_o}{R_1 C_2} \times \frac{1}{s_1 - s_2} \left[\frac{1}{s - s_1} - \frac{1}{s - s_2}\right] \tag{25}$$

where s_1 and s_2 are the roots of the equation $s^2 + as + b = 0$ and both will be negative.

Taking inverse Laplace transform of equation (25)

$$e(t) = \frac{V}{R_1 C_2\,(s_1 - s_2)} [e^{s_1 t} - e^{s_2 t}] \tag{26}$$

In the practical case R was much greater than R_1 and C_1 was much greater than C_2 and an approximate solution could be obtained by examining the auxiliary equation:

$$s^2 + (\frac{1}{R_1C_1} + \frac{1}{RC_2} + \frac{1}{R_1C_2})s + \frac{1}{RR_1C_1C_2} = 0 \qquad (27)$$

where the value of $(\frac{1}{R_1C_1} + \frac{1}{RC_2})$ is much smaller than $\frac{1}{RC_2}$

The equation (27) becomes

$$s^2 + (\frac{1}{R_1C_1})s + \frac{1}{RR_1C_1C_2} = 0$$

and the roots will be

$$s_1 \simeq -\frac{1}{R_1C_2}$$

$$s_2 \simeq -\frac{1}{RC_1}$$

and

$$|s_1| \gg |s_2|$$

The equation for the output voltage then becomes

$$e(t) = V_o[e^{-\frac{t}{RC_1}} - e^{-\frac{t}{R_1C_2}}] \qquad (28)$$

and the graph of the expression is shown in Figure 20. Substituting the actual values of capacitaries and resistors in equation (28) the expression becomes

$$e(t) = V_o[e^{-.0387t} - e^{-2.52t}]$$

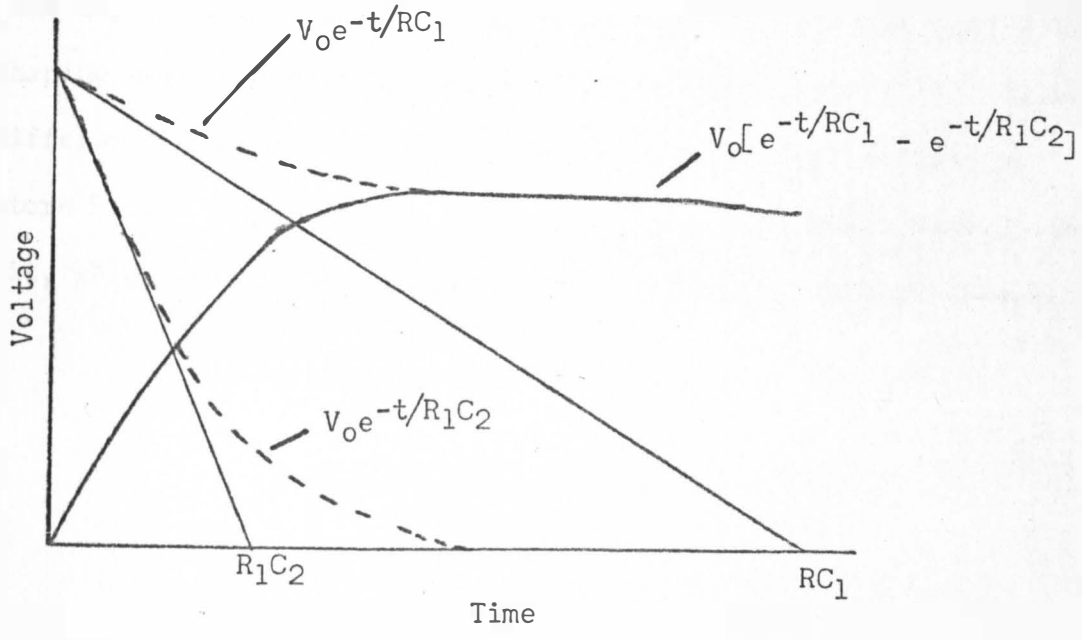

Fig. 20. The impulse voltage wave and its components.

B. Practice

The value of resistors R_1 and R_5 of the waveshaping circuit were found out by estimate and try method. The calculated value of resistors R_1 and R_2 were taken as the starting values and the waveshape was observed on the oscilloscope type 507 and pictures of waveforms were taken with the help of attached oscilloscope camera. Various values of resistors were used until an exact $1\frac{1}{2} \times 40\mu$sec. waveshape was observed on the oscilloscope. Resistors R_1 and R_2 are non-inductive wire wound resistors. The final values of R_1 and R_2 were 160 ohms and 2,900 ohms, respectively. These values are the same as used by Keith E. Crouch in

his thesis entitled "The Effect of Waveshape on the Electric Breakdown of Nitrogen Gas".[16]

The experimentally determined values of resistors were used in the waveshaping circuit while conducting the breakdown tests. The reason for the difference between the theoretical and experimental values for resistors R_1 and R_2 was due to stray capacitance and inductance in the circuit, which were not accounted in the mathematical calculations.

APPENDIX IV

VOLTAGE CALIBRATION OF THE IMPULSE GENERATOR

The panel meter on the control cabinet of the impulse generator does not give the direct reading of the impulse voltage present at the test cell. Therefore, the panel meter on the control cabinet must calibrate against the actual kV output of the generator. The procedure used in the calibration of the impulse generator is recommended by AIEE Standards # 4.[17] The generator output is controlled by the control knob on the panel. The voltage calibration is carried out by two methods; oscilloscope deflection measurement method and the use of sphere gaps in flashover tests. The AIEE Standards[17] requires that the difference between the two methods readings should not exceed 5 percent of the lower value.

The Cathode Ray Oscilloscope was obtained by using the oscilloscope deflection. The resistance divider having wire wound resistors was used as prescribed by the same standards. The equation derived for obtaining the actual generator output voltage in terms of the oscilloscope deflection follows:

$$E = \frac{(\text{scope deflection in cm.})}{(\text{attenuation})} \times \frac{50 \text{ volts}}{\text{cm.}} \times \frac{R_2 + \dfrac{R_3 \times R_4}{R_3 + R_4}}{\dfrac{R_3 \times R_4}{R_3 + R_4}} \times 10^{-3} \quad (1)$$

Where E is the peak voltage at the test cell, R_2 and R_3 are the resistors used in the wave shaping circuit and R_4 is the input resistance of the oscilloscope type 507. The attenuation is the percentage of the

input scope signal applied to the vertical deflection plates of the oscilloscope. Substituting the various known values in equation (1), the equation becomes

$$E = \frac{\text{scope deflection in cm.}}{\text{attenuation}} \times 3.95 \text{ kV} \qquad (2)$$

The above equation was used in calibrating the actual output voltage against the panel meter reading. At different panel meter settings, the oscillograms were taken and the oscilloscope deflection was measured. Substituting the measured quantities in equation (2), the output voltage was calculated and entered in Table 9. Figure 21 shows the plot of output voltage against panel meter reading.

TABLE 9. Measurement and Calculation of Output Voltage of the Impulse Generator on the Type 507 Oscilloscope With Positive Polarity for a $1\frac{1}{2} \times 40\,\mu$sec. Wave.

Panel Meter Setting	Attenuation on Oscilloscope	Scope Deflection	Generator Output Voltage
μA		cm.	kV
3.5	1.0	1.85	7.32
5.0	1.0	2.55	10.05
6.0	1.0	3.05	12.05
7.0	1.0	3.60	14.20
8.0	1.0	4.15	16.40
9.0	1.0	4.65	18.40
10.0	1.0	5.10	20.10
11.0	0.8	4.50	22.20
12.0	0.8	4.90	24.10
13.0	0.8	5.35	26.30
14.0	0.7	5.0	28.20
15.0	0.7	5.35	30.20
16.0	0.6	4.90	32.25

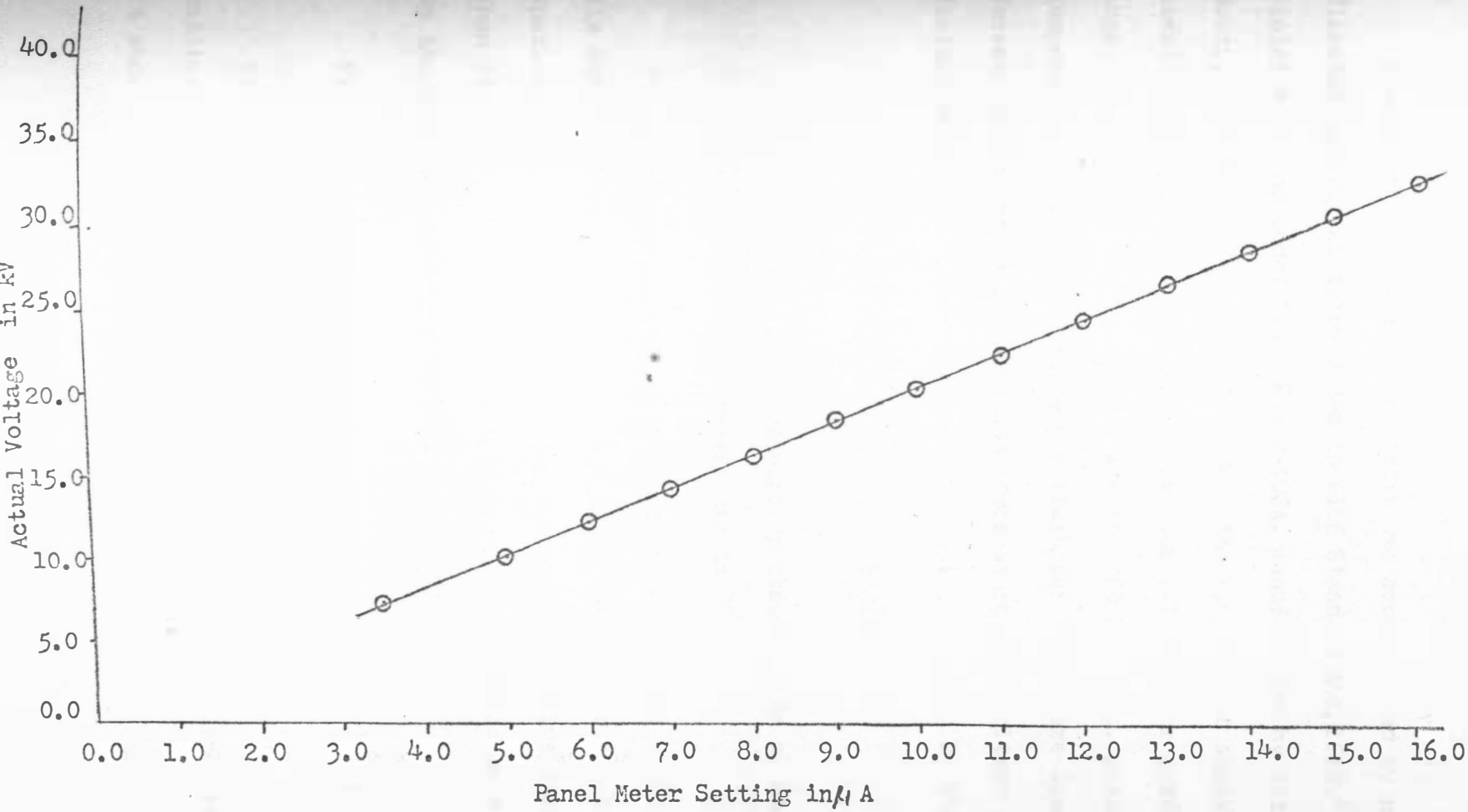

Fig. 21. The Calibration Curve of the Impulse Generator by the Oscilloscope Deflection Method for $1\frac{1}{2} \times 40$ μsec. Positive Polarity Wave Shape.

The sphere gap calibration tests was accomplished by using 6.25 cm diameter spheres as recommended in AIEE Standard #4, 1953.[17] The ultraviolet ray lamp model Black Ray B-100A, manufactured by Ultraviolet Products, California, was used to reduce the time lag of sparkover and to obtain consistent results. The sparkover voltages for different spacings, as given in the Standards, are for 760 mm of Hg. pressure and 25°C temperature. Since the sphere gap flashover tests were done under different conditions of pressure and temperature, the voltage correction factors were used. The relative air density is given by the relation

$$\text{Relative Air Density} = \frac{0.392b}{273 + t}$$

where b = barometric pressure in mm of Hg.

t = temperature in °C.

The corresponding voltage correction factors for various relative air densities were taken from Table II of the Standards. To obtain sparkover value for a specified gap spacing at relative density other than standard, the voltage obtained from the Standards were multiplied by the voltage correction factor, i.e.

$$kV_{test} = (kV_{standard} \times \text{Voltage Correction Factor}) \text{ for a given spacing}$$

The sphere gaps flashover test data are shown in Table 10. The calibration curve, sphere gap flashover voltage vs. panel meter reading is shown in Figure 22.

TABLE 10. The Sphere Gap in Flashover Test Datas.

Panel Meter Setting	Gap Spacing	Gap Spark-over from Calibration Curve kV Crest	Pressure at Gap	Temperature at Gap	Relative Air Density	Voltage Correction Factor	Gap Spark-over Kilo-Volts Crest	Voltage from Oscille-scope Calibrat-ion Curve	Error
μA	cm.	kV	mm of Hg.	°C			kV	kV	%
8.0	0.5	17.00	72.60	22.2	0.961	0.968	16.42	16.40	+1.25%
9.0	0.6	19.10	713.5	29.8	0.922	0.929	17.65	18.10	-2.5%
10.0	0.7	22.65	713.5	29.8	0.922	0.929	21.00	20.10	-0.5%
11.0	0.8	23.60	713.9	24.8	0.939	0.946	23.6	22.20	+6.1%
12.25	0.9	28.28	713.9	24.8	0.939	0.946	29.1	26.60	+6.80
15.0	1.1	33.50	713.9	24.8	0.939	0.946	31.6	30.20	+4.62
17.0	1.25	38.20	715.8	24.8	0.940	0.946	36.0	34.30	+5.00

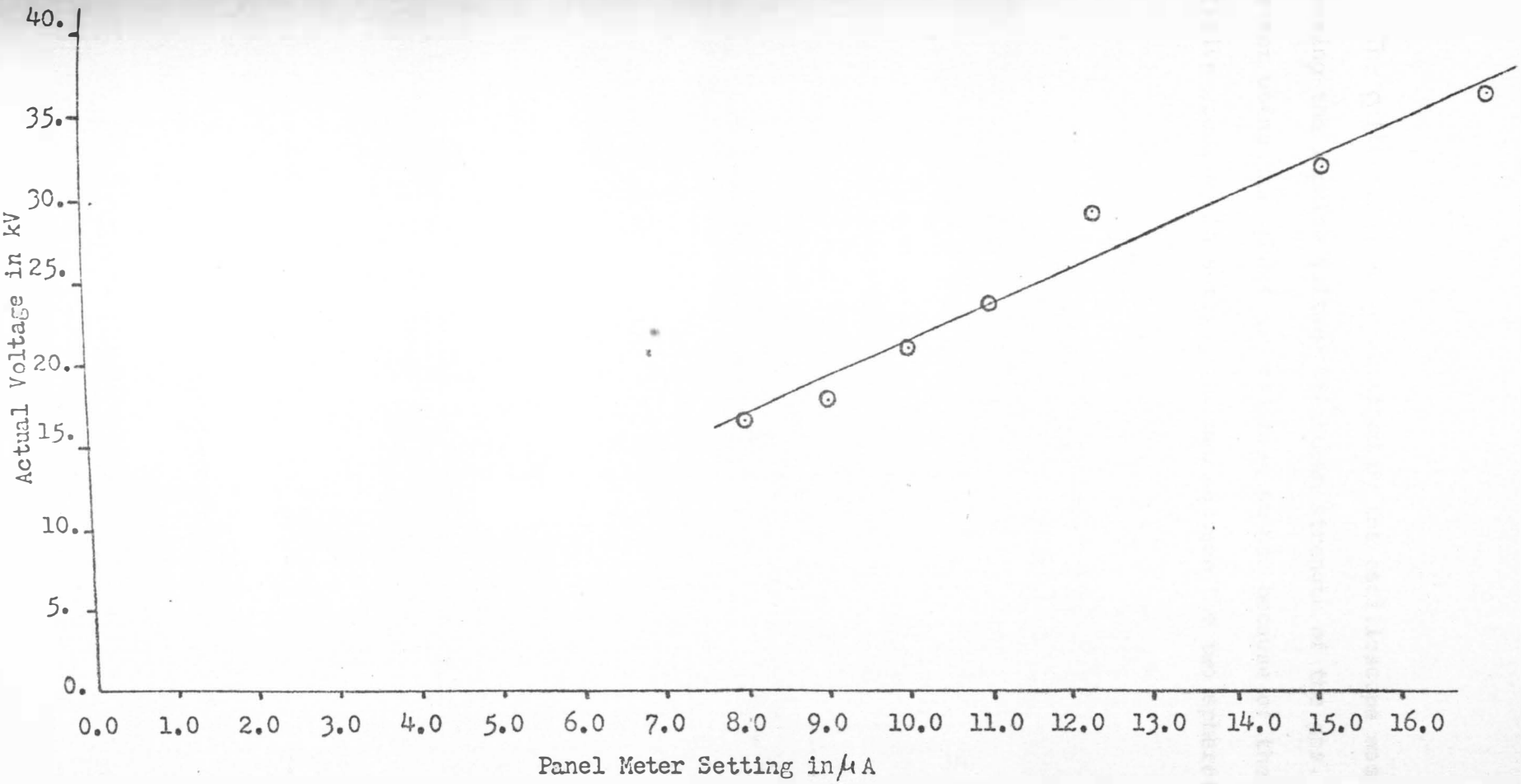

Fig.22. The Calibration Curve of the Impulse Generator by the Sphere Gap in Flashover Test Method for $1\frac{1}{2} \times 40\,\mu$sec. Positive Polarity Wave Shape.

The calibration curve obtained by the oscilloscope was used in plotting the impulse voltage breakdown strength of the gas. The reason for not using the sphere gap calibration was because of the lack of relative accuracy in setting the gap between the two spheres.

APPENDIX V

ADJUSTMENT OF THE GAS IN THE CELL TO STANDARD CONDITIONS

The breakdown voltage of any gas for a certain gap setting and electrode system varies with the pressure and temperature of the gas inside the test cell. Therefore, it is necessary to fill the test cell under a certain pressure and temperature, i.e., to insure that number of moles of gas inside the test cell are the same at every filling. Since the pressure and temperature of the room varies from day to day, some means has to be found to take into account this change in pressure and temperature. It is practically not possible to maintain the pressure and temperature of the room constant. However, pressure of the gas inside the test cell can be conveniently controlled. An equation can be developed which determines the required pressure inside the test cell in terms of room pressure and temperature to take into account the difference between ambient and standard conditions. This is done as follows:

Always, the pressure inside the test cell was nearly equal to one atmosphere and the temperature of the gas was 55°C or more above the boiling point of C_3F_8 gas. Thus, it can be safely assumed that C_3F_8 gas was subjected to ideal filling conditions. It then follows that the universal gas law is applicable, i.e.

$$\frac{P_t V_c'}{T_t} = \frac{P_s V_c}{T_s} \tag{1}$$

where

P_t = Pressure of gas inside the test cell in inches of Hg. at any temperature T_t ^{o}R.

P_s = Any specified standard pressure of gas inside the cell under specified standard temperature T_s ^{o}R.

$V_{c'}$ = Inside volume of test cell at temperature T_t ^{o}R.

V_c = Inside volume of test cell at temperature T_s ^{o}R.

It should be noted that number of moles of gas inside the cell were the same under existing conditions. The change in volume of the test cell was assumed to be negligible when heated to the highest temperature. Therefore, it follows:

$$V_{c'} = V_c$$

The equation (1) can be rewritten as

$$\frac{P_t}{T_t} = \frac{P_s}{T_s} \tag{2}$$

or

$$P_t = P_s \times \frac{T_t}{T_s} \tag{3}$$

From equation (3), it can be interpreted that P_t is the required pressure of gas inside the test cell. This insures that the number of moles inside the test cell is the same as though it were filled under specified conditions.

Let the room pressure and temperature be P_A inches of Hg. and T_A ^oR. If the cell were filled at room temperature then it follows that

$$T_t = T_A$$

The equation (3) can be rewritten as

$$P_t = P_s \times \frac{T_A}{T_s}$$

Therefore, in order to maintain the same number of moles of gas, the test cell should be filled at pressure $(P_t - P_A)$ above the room pressure. The pressure change needed is

$$\Delta P = P_t - P_A = [P_s \times \frac{T_A}{T_s} - P_A] \qquad (5)$$

where ΔP was the pressure change required in inches of Hg.

The specified standard conditions were assumed to be

$$P_s = 28.35\text{" of Hg.}$$

$$T_s = 80^oF \text{ or } (460 + 80)^oR$$

Substituting these values in equation (5)

$$\Delta P = [28.35 \times \frac{(T_A + 480)}{(480 + 80)} - P_A]$$

if T_A was expressed in ^oF.

The leveler tubes used to change the pressure inside the test cell were filled with Silicone Oil which had a density of 0.870 gm/cc.

It is known that Pressure = density time height. Since mercury has a density of 13.60 gm/cc, it follows that 1.0" of mercury column

height is equal to $\frac{13.60}{0.870}$ = 15.66" of Silicone Oil column. Therefore, if ΔP is expressed in inches of Silicone Oil, equation (6) becomes:

$$\Delta P = 15.66 \times \left[28.35 \times \frac{(T_A + 480)}{(480 + 80)} - P_A\right] \text{ inches of Silicone Oil}$$

Equation (7) gives the difference between the level of Silicone Oil in the leveler tubes of Figure 6. The positive sign on ΔP would indicate that the level in the leveler tube L_1 should be lower than the tube L_2 and vice versa for a negative sign on ΔP. Thus, it is possible to calculate the required pressure change inside the test cell, above or below the room pressure, by using equation (7). This procedure insures the same number of moles at every filling.

APPENDIX VI

DETERMINATION OF THE THERMAL LINEAR EXPANSION OF THE TEST CELLS

The test cells were heated to a relatively high temperature in the oven before the electric breakdown tests were made. Expansion of the cell material at high temperature creates changes in the electrode system gap spacing. Correction for lower to higher gap spacings must be made. This was done by two methods, theory and practice.

Theory

The change in the length ΔL is given by the following relation:

$$L = L_o . \alpha . \Delta T \qquad (1)$$

where

L is the original length

L_o is the linear co-efficient of thermal expansion

α is the change in temperature

The test cells are made of various materials and are considered as a composite body. The change in length of various components was calculated and added to estimate the total expansion of the cell.

A. Linear expansion of test cell with sphere to plane electrode system (South Dakota State University # 56667)

The electrode system is made of steel and brass. Moreover, expansion of the pyrex glass wall was measured and the linear co-efficient of thermal expansion for the different materials were taken from the Physi-Tables. For different materials, the calculation was carried out as follows. First, assumed temperature rise of 100°C and a gap setting of 100 mills.

1. For Steel:

$L_o = 5.536$ inches

$\alpha = 1.2 \times 10^{-5}$ inches/^oC

$\Delta T = 100.0^oC$

$\Delta L = L_o \alpha \Delta T$

$= (5.536) \times (1.2 \times 10^{-5}) \times (100.0) = 0.00665$ inches

2. For Brass:

$L_o = 2.407$ inches

$\alpha = 2.02 \times 10^{-5}$ inches/^oC

$\Delta T = 100.0^oC$

$\Delta L = L_o \alpha \Delta T$

$= (2.407) \times (2.02 \times 10^{-5}) \times (100.0) = 0.00485$ inches

3. For Pyrex Glass:

$L_o = 8.0$ inches

$\alpha = 0.33 \times 10^{-5}$ inches/^oC

$\Delta T = 100^oC$

$\Delta L = (8.0) \times (0.33 \times 10^{-5}) \times (100.0)$

$= 0.00265$ inches

The change of gap spacing with a temperature increase of 100^oC is given by:

ΔL_G = (increase in metal length) - (increase in glass length)

$= [(0.00665 + 0.00485) - (0.00265)]$ inches

$= 0.00885$ inches

Therefore, the gap spacing decreases by the above amount for 100°C temperature rise.

Now $$\frac{\Delta L_G}{\Delta T} = \frac{0.0085}{100.0} \text{ inches}/^{\circ}C$$

$$= 8.85 \times 10^{-2} \text{ mils}/^{\circ}C$$

B. Linear expansion of the test cell having a point to plane electrode system (South Dakota State University # 53508)

The calculation for this cell was carried out in the same way as follows:

1. For Steel:

$L_o = 4.925$ inches

$\alpha = 1.2 \times 10^{-5}$ inches / °C

$\Delta T = 100.0^{\circ}C$

$\Delta L = (4.925) \times (1.2 \times 10^{-5}) \times 100$ inches

$= 0.0059$ inches

2. For Brass:

$L_o = 1.625$ inches

$\alpha = 2.02 \times 10^{-5}$ inches °C

$\Delta T = 100.0^{\circ}C$

$\Delta L = (1.625) \times (2.02 \times 10^{-5}) \times (100.0)$ inches

$= 0.0033$ inches

3. For Pyrex Glass:

$L_o = 7.937$ inches

$\alpha = 0.33 \times 10^{-5}$ inches / ^oC

$\Delta T = 100.0^oC$

$\Delta L = (7.937) \times (0.33 \times 10^{-5}) \times (100.0)$ inches

$= 0.0026$ inches

The change of gap spacing L_G with temperature would be

$\Delta L_G = [(0.0059 + 0.0033) - (0.0026)]$ inches

$= 0.0066$ inches

Therefore, the gap spacing decreases by the above amount for 100^oC temperature rise.

Now $$\frac{\Delta L_G}{\Delta T} = \frac{0.0066}{100.0} = 6.60 \times 10^{-2} \text{ mils}/^oC$$

Practice

First, the experimental means of determining the value of $\Delta L_G/\Delta T$ was done as follows: The micrometer reading for sphere to plane electrode was taken for zero gap setting and also the room temperature was recorded. The zero gap setting was called the initial zero reading. Next, the cell was placed in the oven. The cell was heated through a temperature change of about 125^oC. After two hours of heating, the temperature of the oven was again recorded. The oven door was then quickly opened and the gap spacing was adjusted to zero again. The reading of the micrometer was recorded. This was called the final zero reading.

From the above readings, the change in length of the gap would be

$$\Delta L_G = \text{(final zero reading - initial zero reading)}$$

also change in temperature

$$\Delta T = \text{(final temperature - initial temperature)}$$

Now, the value of $\Delta L_G/\Delta T$ for sphere to plane electrode test cell could be easily found. This was the value of a zero gap spacing of the test cell. However, a correction has to be made in the value of $\Delta L_G/\Delta T$ since at 0.1" gap spacing, 0.1" less of steel in the micrometer screw was contributing to the decrease of the gap spacing as compared with the zero gap spacing. The value of $\Delta L/\Delta T$ for 0.1" length of steel was found by theory and was subtracted from the value of $\Delta L_G/\Delta T$ at zero gap setting. This would give the value of $\Delta L_G/\Delta T$ at 0.1" spacing for sphere to plane electrode system cell. In the same manner the value of $\Delta L_G/\Delta T$ was determined for point to plane electrode cell. These values are shown in the following table.

TABLE 11. The Correction Factor for the Thermal Linear Expansion of the Test Cells.

Type of Test Cell	$\Delta L_G/\ T$ at Zero Spacing	$\Delta L/\ T$ for 0.1" of Steel	$\Delta L_G/\ T$ at 0.1" Spacing
	mils ^oC	mils ^oC	mils ^oC
Sphere to Plane Electrode System Cell	0.0862	0.0020	0.0842
Point to Plain Electrode System Cell	0.0742	0.0012	0.0730

The theory and practice value agreed very closely. However, values by practice were used in the gap setting. In the calculation of the theoretical value, there was doubt about the exact kind of materials in the cells. Also, the effect of expansion of the bolts was neglected.

APPENDIX VII

THERMOCOUPLE CONSTRUCTION AND DETERMINATION OF THE TEST CELL HEATING TIME

A. Thermocouple Construction and Temperature Measurement

The measurement of temperature inside the oven was done by using iron-constantan in thermocouples. The thermocouples wire was covered by glass and asbestos. Ten identical thermocouples were used and position of their hot junctions inside the oven is shown in Figure 23. The leads from the thermocouples were connected to one side of a wood cold junction terminal board. The leads from the other side of the terminal board were connected to a Leeds and Northrup Millivolt potentiometer through an eleven position rotary selector switch. The selector switch has one "off" position whereby the millivolt potentiometer is disconnected from the thermocouples. This "off" position is utilized during the calibration of the potentiometer. The other ten positions on the selector switch permits reading of the thermo-emf developed between the cold and hot junction on any one of the ten thermocouples. The temperature was monitored by an ordinary -20^{o}C to 100^{o}C mercury thermometer positioned directly above the wood terminal board.

The millivolt potentiometer was equipped with a reference (cold junction) compensator. The compensator circuit can be adjusted to develop an equal and opposite voltage at the cold junction. This makes possible a direct reading of emf developed at the hot junctions which are located inside the oven. The emf developed at the hot junction is directly proportional to the temperature of the oven. The Standard

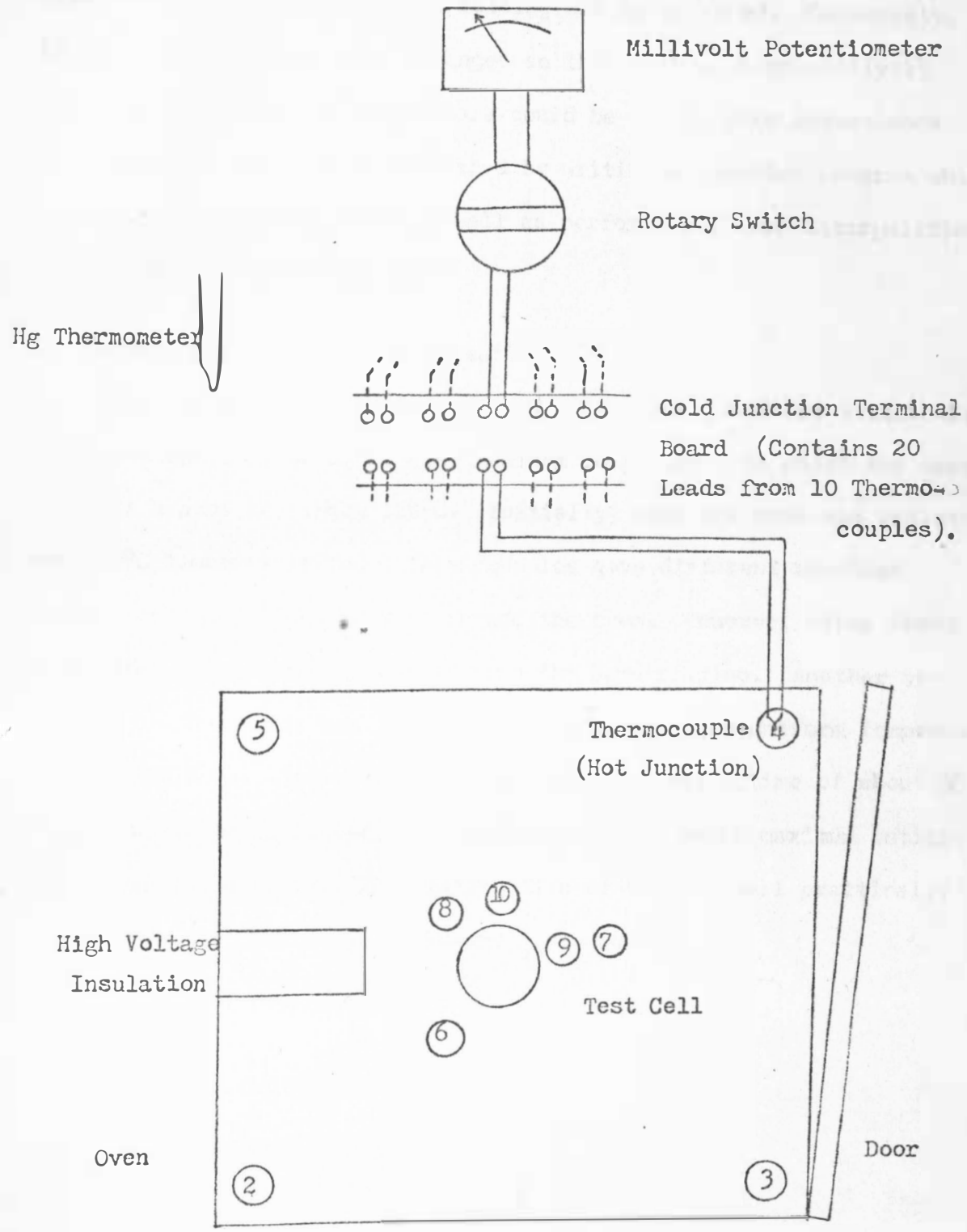

Fig.23. Location of Thermocouples and Thermocouple Circuit Diagram Used to Measure Temperature Inside the Oven.

Table for iron-constant in thermocouples is arranged so that for a given temperature, a millivolt reading can be obtained. Conversely, if the Standard Table were arranged so that with a given millivolt value, a corresponding temperature could be found, more convenience is possible. This was accomplished by writing a computer program which inverted the Standard Table as well as performing linear interpolation between the millivolt values.

B. Determination of Test Cell Heating Time

The ten thermocouples were placed in various locations inside the oven as shown in Figure 23. The maximum temperature to which the test cell was heated was about 150°C. Initially, when the oven was adjusted for 150°C temperature, some thermocouples gave different readings because of non-uniform heating inside the oven. However, after about 50 minutes all the thermocouples gave the same reading. Another allowance of 30 minutes was given for the cell to reach uniform temperature in the oven. The author believes that a heating time of about 80 minutes would be sufficient for the test cell to reach maximum anticipated oven temperature. The heating time of the gas cell practically agrees with the conclusion of Edward J. Roman.[8]